

Chapter 2

Lower rim guanidinium calix[4]arenes for cell transfection[§]

2.1 Introduction

As shown in some examples reported in the **Chapter 1**, referring in particular to the calixarene derivatives, the charged groups of the synthetic vector are constituted by guanidinium units. The guanidinium group, (**Fig. 2.1**) for its structural and physico-chemical properties, is widely used in supramolecular chemistry for the recognition of anionic species. Thanks to resonance structures, the guanidinium group is planar and it stays protonate in a wide range of pH ($pK_a \sim 12.5$). These properties make this group very versatile for the recognition of tetrahedral and Y-shaped ions, complexing them by exploiting the chelate effect. Besides, oligoguanidinium compounds resulted very interesting systems for the cell membrane penetration¹ and for the transport of molecular species associated to it.

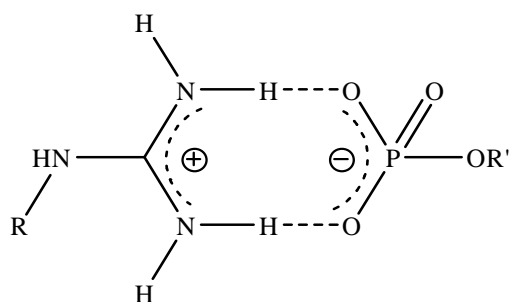


Fig. 2.1. Interaction between the guanidinium group and the phosphate ion.

The main part of my thesis was devoted to improve the efficiency and lower the toxicity of a class of non-viral vectors having guanidinium moieties exposed on calixarene scaffolds, trying also to understand the mechanisms of the transfection process. Previous work showed that calix[*n*]arenes bearing guanidinium groups directly attached on the aromatic nuclei (upper rim)² are able to condense plasmid and linear DNA and perform cell transfection in a way which is strongly dependent on the macrocycle size, lipophilicity and conformation. Unfortunately, these compounds are characterized by low transfection efficiency and high cytotoxicity, especially at the vector concentration required for observing cell transfection (10-20 μM), even in the presence of the helper lipid DOPE (dioleoylphosphatidylethanolamine).³

The first goal of this project was the synthesis of new potential non-viral vectors for gene delivery, based on the calix[4]arene scaffold blocked in the cone conformation, functionalized with cationic guanidinium groups at the lower rim. In particular, this new class presents an inversion of the reciprocal position between the hydrophilic and hydrophobic regions compared to the upper rim guanidinium calixarenes. The aim was to evaluate if this structural

modification would bring better results in DNA condensation and transfection and could reduce the toxicity.

2.2 Results and discussion

The guanidinium moieties were attached to the phenolic OH groups of the calix[4]arene through a three carbon atom spacer and the upper rim was unsubstituted or substituted with *t*-butyl or hexyl chains (**Fig. 2.2**).

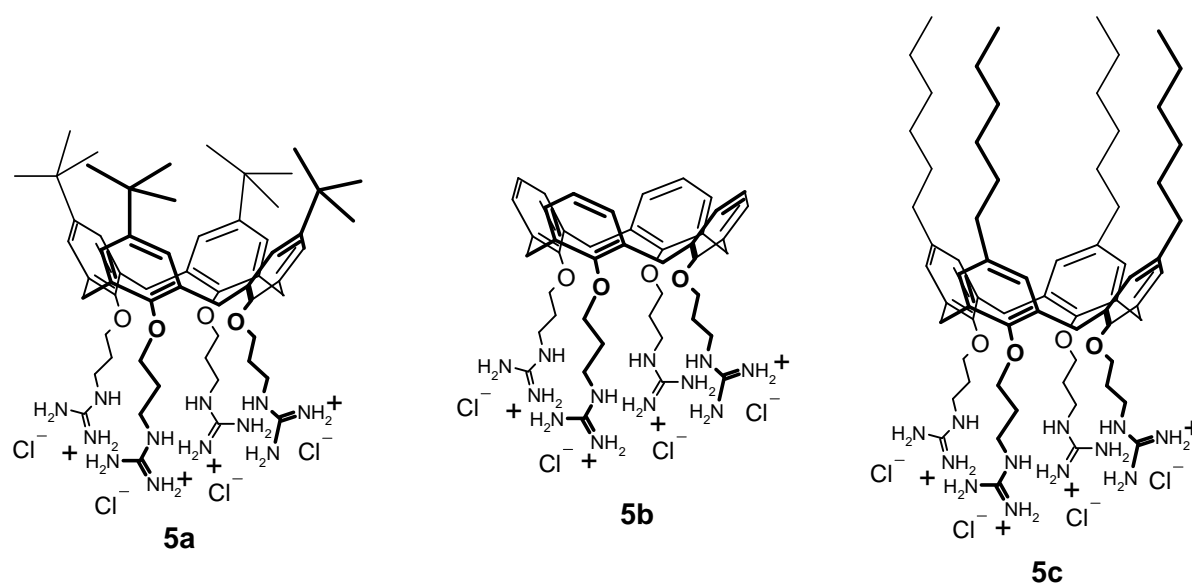
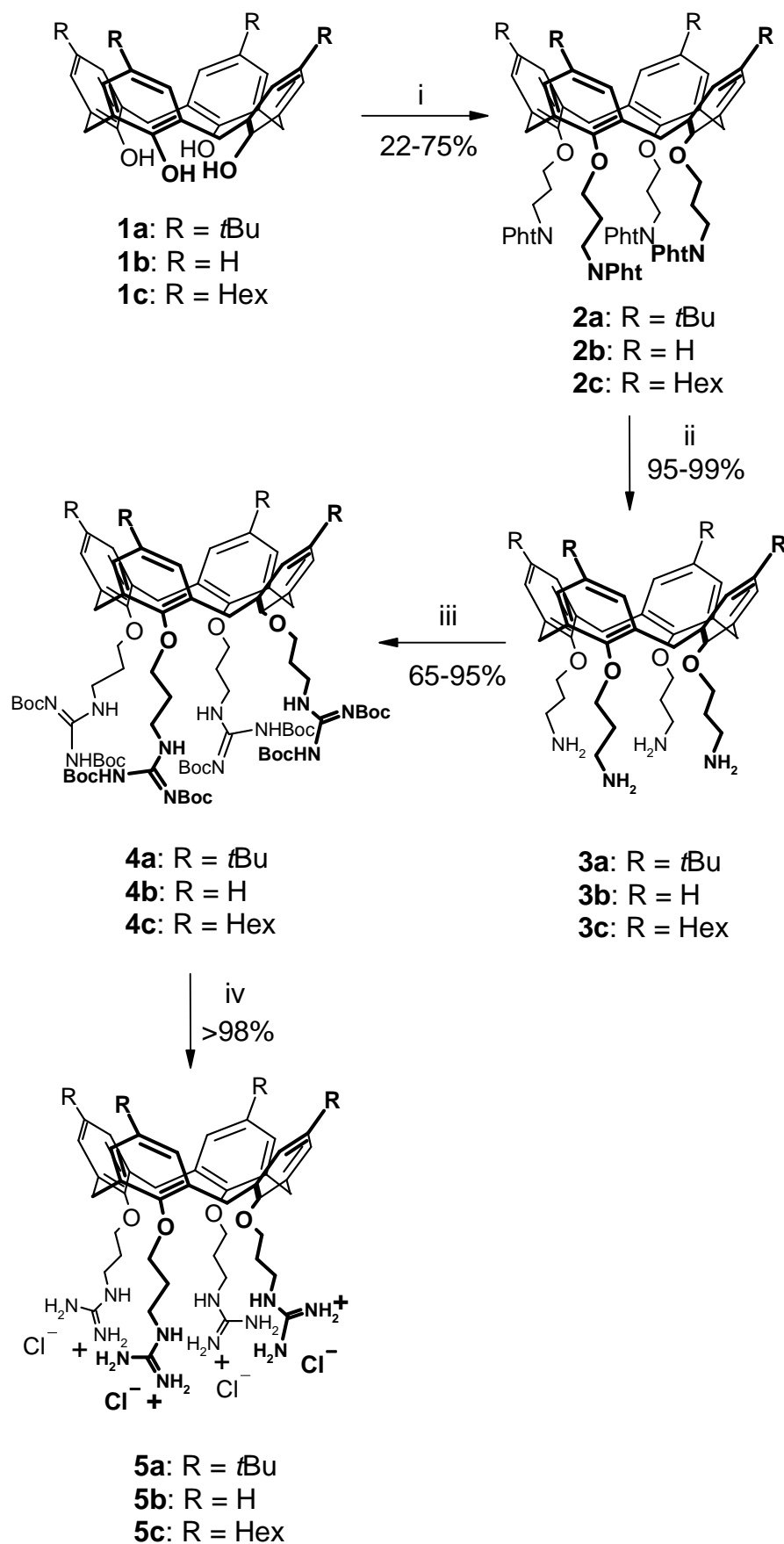


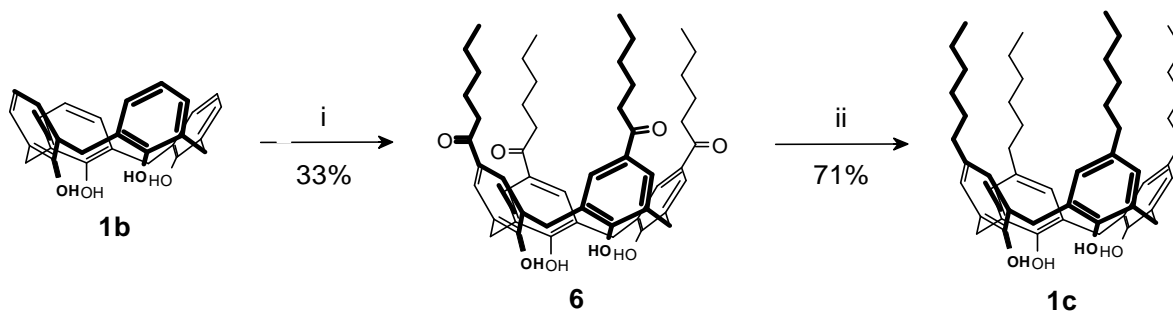
Fig. 2.2. Structural formulas of the lower rim guanidinium calix[4]arenes **5a-c**.

2.2.1 Synthesis of the lower rim guanidinium calix[4]arenes **5a-c**

The three new lower rim guanidinium calix[4]arenes **5a-c** were synthesized in four steps according to **Scheme 2.1**. The starting calix[4]arene platforms **1a,b** are easily available, even from commercial sources, whereas the hexyl derivative **1c** had to be synthesized by acylation of calix[4]arene **1b** at the upper rim with hexanoyl chloride, followed by the reduction of the acyl groups (**Scheme 2.2**). The hexanoyl chloride was obtained treating the hexanoic acid with (COCl)₂ in dry CH₂Cl₂ using DMF as catalyst.⁴



Scheme 2.1. Synthesis of the lower rim guanidinium calix[4]arenes **5a-c**. i) N-(3-bromopropyl)phthalimide, NaH, dry DMF, N₂, rt; ii) NH₂NH₂·H₂O, abs EtOH, N₂, reflux; iii) N,N'-di-Boc-N''-triflylguanidine, CH₂Cl₂ (for **4a** and **4b**), N₂, rt; CHCl₃ (for **4c**), N₂, rt; iv) HCl 37%, 1,4-dioxane, rt.



Scheme 2.2. Synthesis of the p-hexyl guanidinium calix[4]arene **1c**. i) hexanoyl chloride, AlCl_3 , nitrobenzene, N_2 , rt; ii) CF_3COOH , $\text{HSi}(\text{C}_2\text{H}_5)_2$, rt.

The reduction of the acyl-derivative **6** was performed using $\text{HSi}(\text{C}_2\text{H}_5)_3$ in CF_3COOH .⁵ However, in these conditions the reaction was not complete even after a very long reaction time and excess of silane, so column chromatography was necessary to obtain the pure compound **1c**. The calix[4]arenes **1a-c** were then reacted (see **Scheme 2.1**) with N-(3-Bromopropyl)-phthalimide in dry DMF, in the presence of NaH as base. The use of this base is necessary to deprotonate all the OH groups and to block the calix[4]arene in the desired cone conformation,⁶ which for calix[4]arenes **2a-c** was proved by examining the ^1H NMR spectra. The phthalimides were then removed in presence of hydrazine to leave the amines **3a-c**.⁶ All the operations necessary for the work-up were done very quickly, to avoid a reaction between the amino groups and the atmospheric CO_2 , originating carbamates that would prevent the further functionalization of **3a-c** (see **Paragraph 2.4**). The amino groups were then functionalized with Boc protected guanidines through reaction with N,N'-di-Boc-N''-triflylguanidine in chloroform or CH_2Cl_2 ,^{6a} to obtain **4a-c**. Finally the guanidine groups were deprotected with HCl 37% in 1,4-dioxane to obtain **5a-c**.^{6a} This reaction needed some days to be completed and it was monitored by mass spectrometry. All the compounds obtained, including intermediates, were characterized by ^1H NMR, ^{13}C NMR and ESI-MS.

Compounds **5a-c** resulted water soluble, an important feature for their use in biological systems. The ^1H NMR spectra in D_2O of compounds **5a** and **5b** at room temperature show sharp signals, at least up to a concentration of 5 (**Fig. 2.3**) and 10 mM (**Fig. 2.4**), respectively. On the contrary broadening is observed for **5c**, indicating significant aggregation favoured by its higher amphiphilic character. At 5 mM and at room temperature the signals are so broad that they often span few ppm, whereas at 363 K, although are still rather broad, they can be assigned unequivocally (**Fig. 2.5**). Nevertheless, at the very low concentration (10^{-5} M) used in the biological studies, no aggregation was taken into account also for this compound.

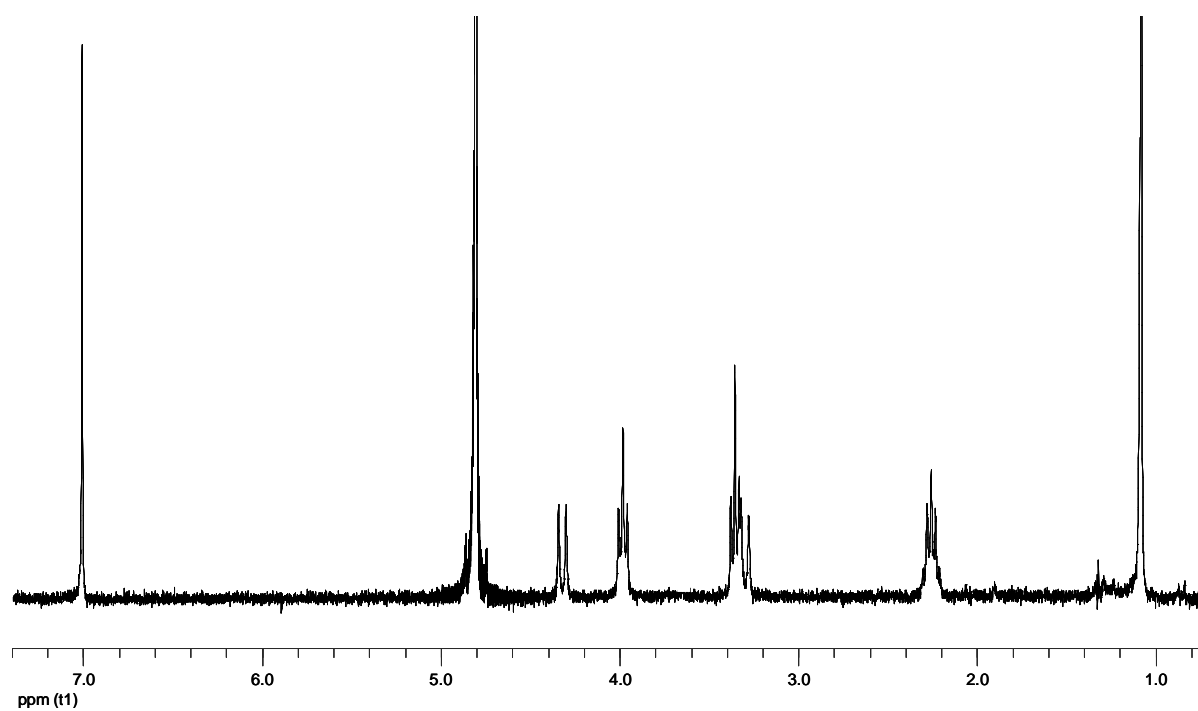


Fig. 2.3. ^1H NMR spectrum (D_2O , 300 MHz, 298 K) of **5a**.

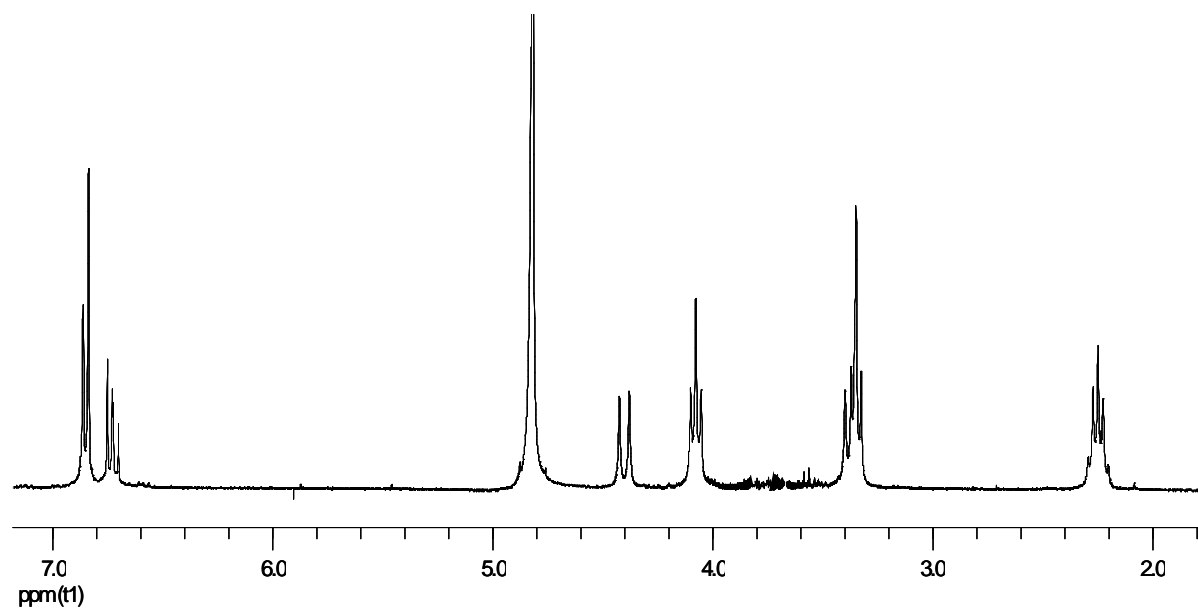


Fig. 2.4. ^1H NMR spectrum (D_2O , 300 MHz, 298 K) of **5b**.

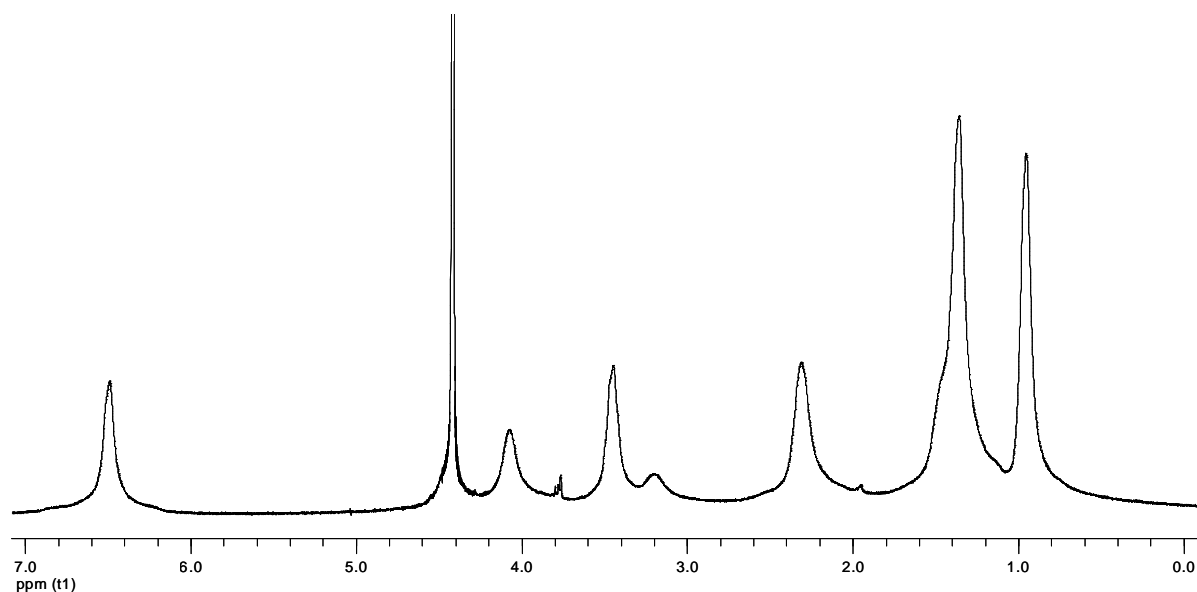


Fig. 2.5. ^1H NMR spectrum (D_2O , 300 MHz, 363 K) of compound **5c**.

The spectrum of **5c** registered in CD_3OD (**Fig. 2.6**) shows well resolved peaks and allows the complete assignment for all signals and the definitive identification of the molecule.

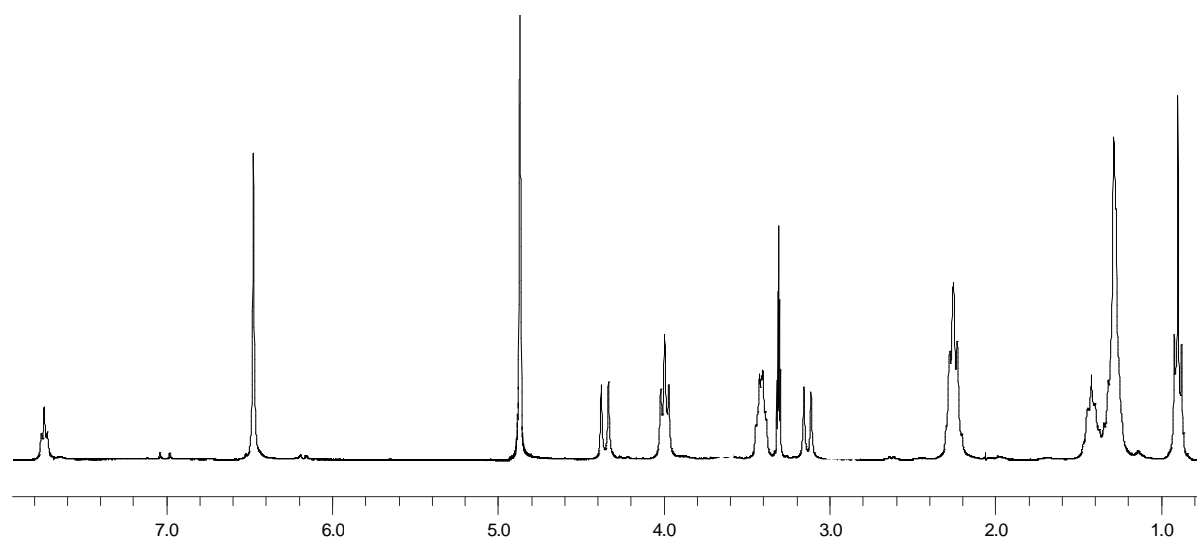


Fig. 2.6. ^1H NMR spectrum (CD_3OD , 300 MHz, 298 K) of compound **5c**.

2.2.2 Gemini-type derivatives

After the synthesis of the calixarenes **5a-c**, it was considered interesting to synthesize a series of Gemini-type compounds, analogues of both the upper and lower rim guanidinium calix[4]arenes, in order to compare the properties of the two classes of derivatives (Calixarenes and Gemini-type) and to try to understand if the macrocyclic structure and the multivalency could play an important role in the biological properties to be studied. The three

lower rim guanidinium Gemini-type compounds **14a-c** (Fig. 2.7) are composed by two apolar phenolic units and two charged guanidinium groups at the end of the two propyl tails, while the upper rim derivative **25** has the two apolar phenolic units derivatized with charged guanidinium groups and apolar hexyl tails (Fig. 2.7).

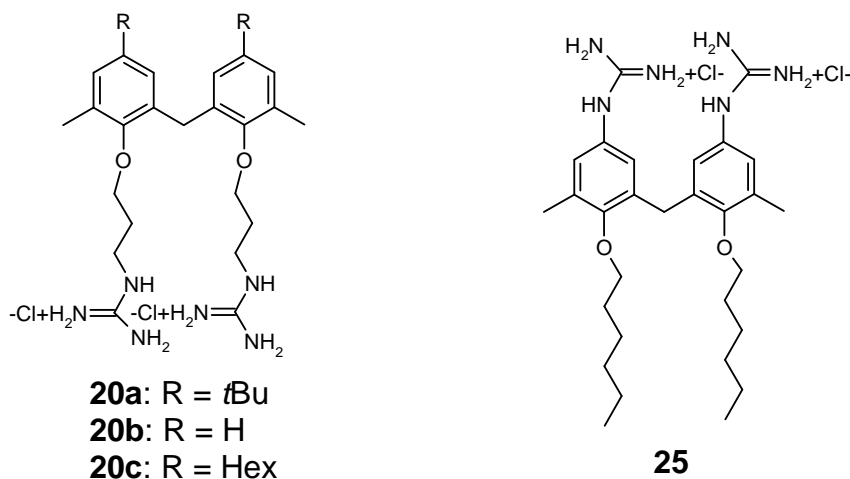
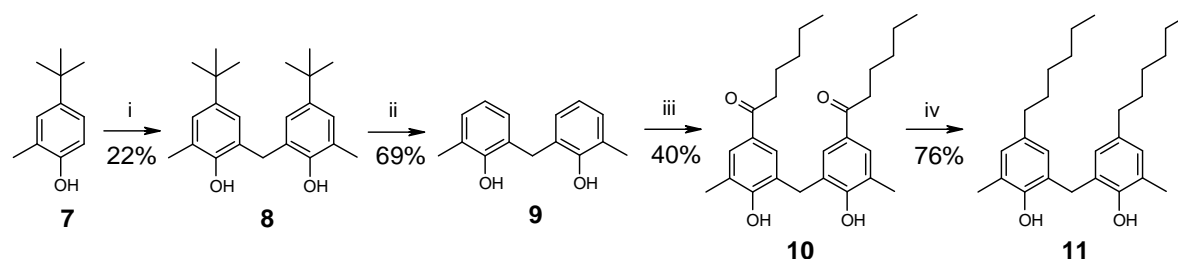


Fig. 2.7. Structural formulas of the synthesized lower and upper rim guanidinium Gemini-type compounds.

2.2.2.1 Synthesis of the lower rim Gemini-type analogues

The synthetic strategy used for the preparation of lower rim Gemini compounds started with the preparation of the corresponding bis[(2-hydroxy-3-methyl)phenyl]methane reagents (Scheme 2.3). The first step was the formaldehyde-phenol condensation using 4-*tert*-butyl-2-methylphenol (**7**). The presence of the methyl and *tert*-butyl groups in positions 2 and 4, respectively, of the phenol nucleus, is also necessary to avoid a polycondensation reaction. Since the procedure reported by Shinkai et al.,⁷ which uses NaOH to transform the phenol into its sodium salt, failed to give the desired diphenylmethane derivative **8**, we performed the condensation reaction using the phoxymagnesium bromide derivative of phenol **7**⁸ obtaining **8** in 22% yield.



Scheme 2.3. Synthesis of the Gemini compounds **8-9-11**. i) 1) EtMgBr, dry THF; 2) paraformaldehyde, toluene, N₂, 120 °C; ii) AlCl₃, dry toluene, rt; iii) hexanoyl chloride, AlCl₃, nitrobenzene, N₂, 50-70 °C; iv) CF₃COOH, HSi(C₂H₅)₂, rt.

De-tert-butylation reaction to obtain compound **9** occurred treating **8** with AlCl_3 , in dry toluene.⁷ Similarly to the procedure used for the calix[4]arene series, introduction of the chains at the aromatic nuclei was obtained through an aromatic acylation of the diphenylmethane **9** onto the 5 and 5' positions with hexanoyl chloride, which was performed by heating the reaction mixture first at 50 °C, and then at 70 °C.⁷ The product **10** was obtained in 40% yield, after purification by column chromatography. A previous attempt to perform the reaction at room temperature, as successfully done with calix[4]arene **1c**, gave the pure product only in 20% yield, again after a column chromatography purification, to remove several by-products (**12-16b**) (**Fig. 2.8**), subsequently characterized by ESI-MS and ^1H NMR. ^1H NMR was particularly useful to distinguish molecules with the same molecular weight.

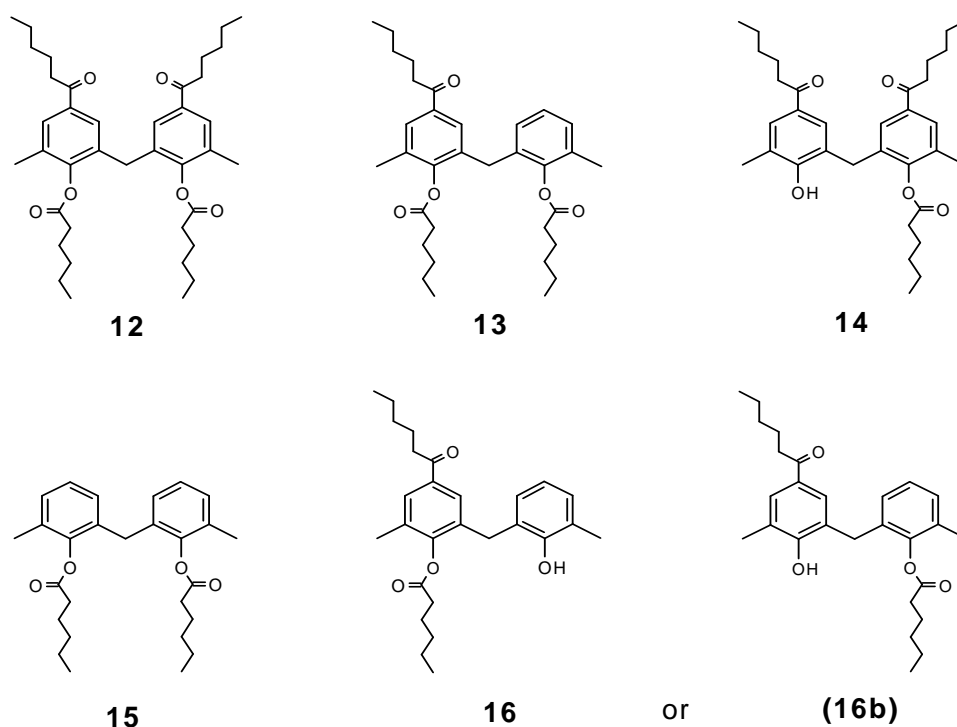
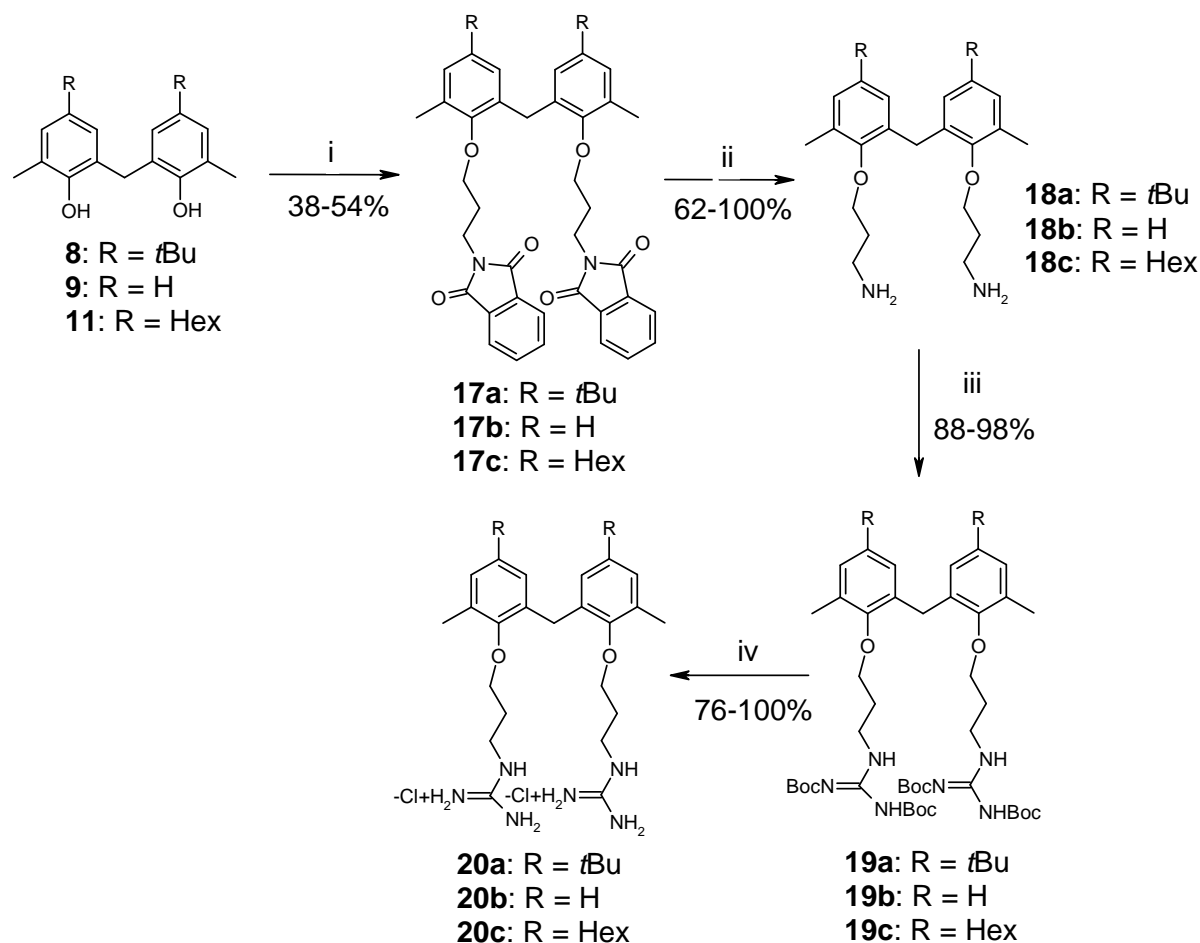


Fig. 2.8. By-products of the Gemini acylation at room temperature.

At this point, the 2,2'-dihydroxydiphenylmethane derivatives **8**, **9** and **11** underwent the same reactions (i-iv, **Scheme 2.4**) used for the calix[4]arene analogues, to produce **20a-c**.



Scheme 2.4. Synthesis of the lower rim Gemini **20a-c**. i) N-(3-bromopropyl)phthalimide, NaH, dry DMF, N₂, rt; ii) NH₂NH₂·H₂O, abs EtOH, N₂, reflux; iii) N,N'-di-Boc-N''-triflylguanidine, Et₃N, CH₂Cl₂, N₂, rt; iv) HCl 37%, 1,4-dioxane, rt.

Crystals of **17b**, suitable for X-ray diffraction analysis, were obtained by fast evaporation of a dichloromethane solution[§] (**Fig. 2.9**). Even if this is not the final compound, it is possible to obtain some interesting indications on the way in which the two aromatic rings of the phenolic groups are reciprocally oriented in this series. The torsion angle C1A-C2A-C20A-C6B (**Fig. 2.10**) is of 116.72(3)° and the two least-squares planes passing through the two benzene rings form an angle of 89.30(5)°. A similar orientation can be also hypothesized for the final product, where the presence of the charged guanidinium groups instead of the phthalimido moieties should induce a similar repulsion of the two halves of the molecule.

[§] The structure was determined by Prof. Franco Ugozzoli at the Department of General and Inorganic Chemistry of this University.

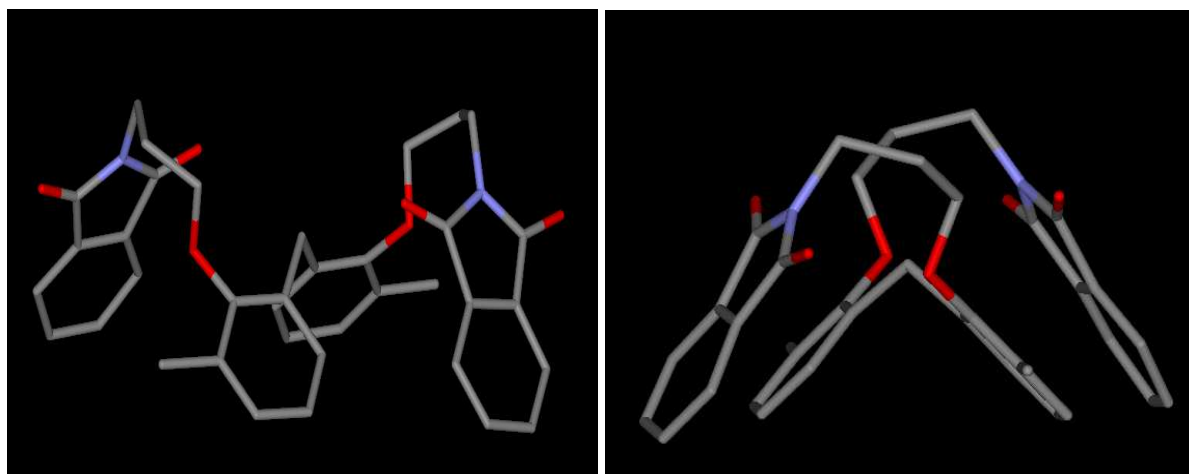


Fig. 2.9. Two perspectives views of the molecular structure of compound **17b** showing the pseudo C_2 symmetry. Hydrogen atoms have been omitted for clarity. Colours are as follows: C, grey; N, blue; O, red.

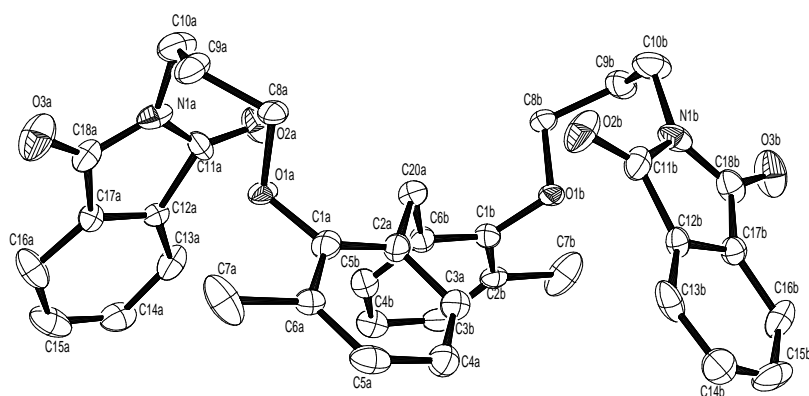


Fig. 2.10. Ortep view (20% ellipsoid probability) of the compound. Hydrogen atoms are omitted for clarity.

Molecular modelling calculation on **20b** supported this hypothesis as shown in **Fig. 2.11**.

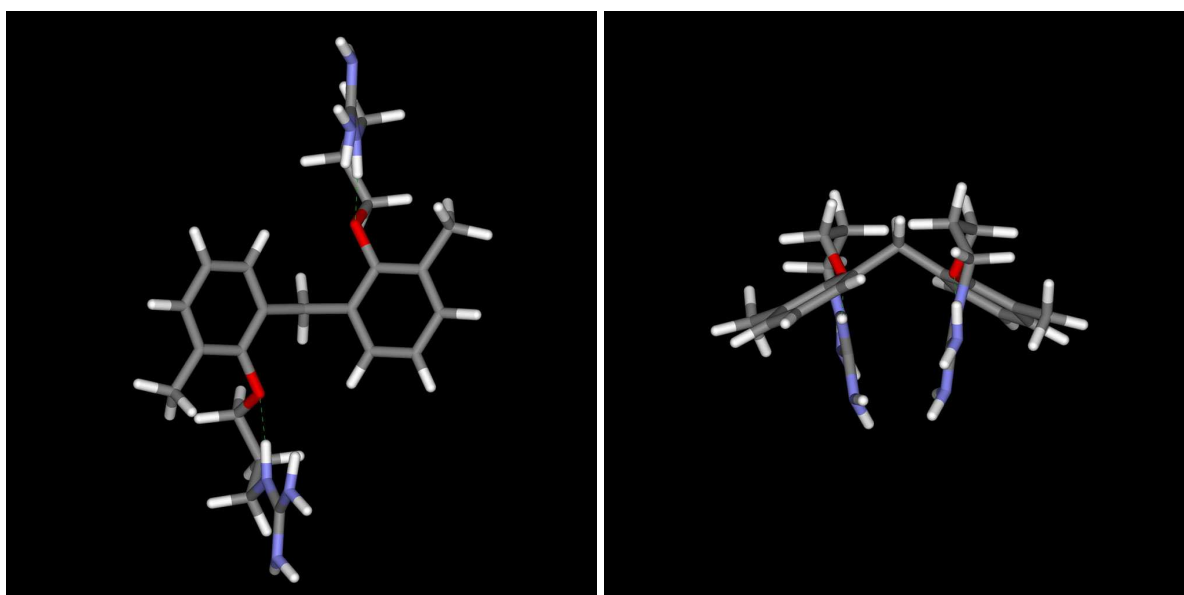
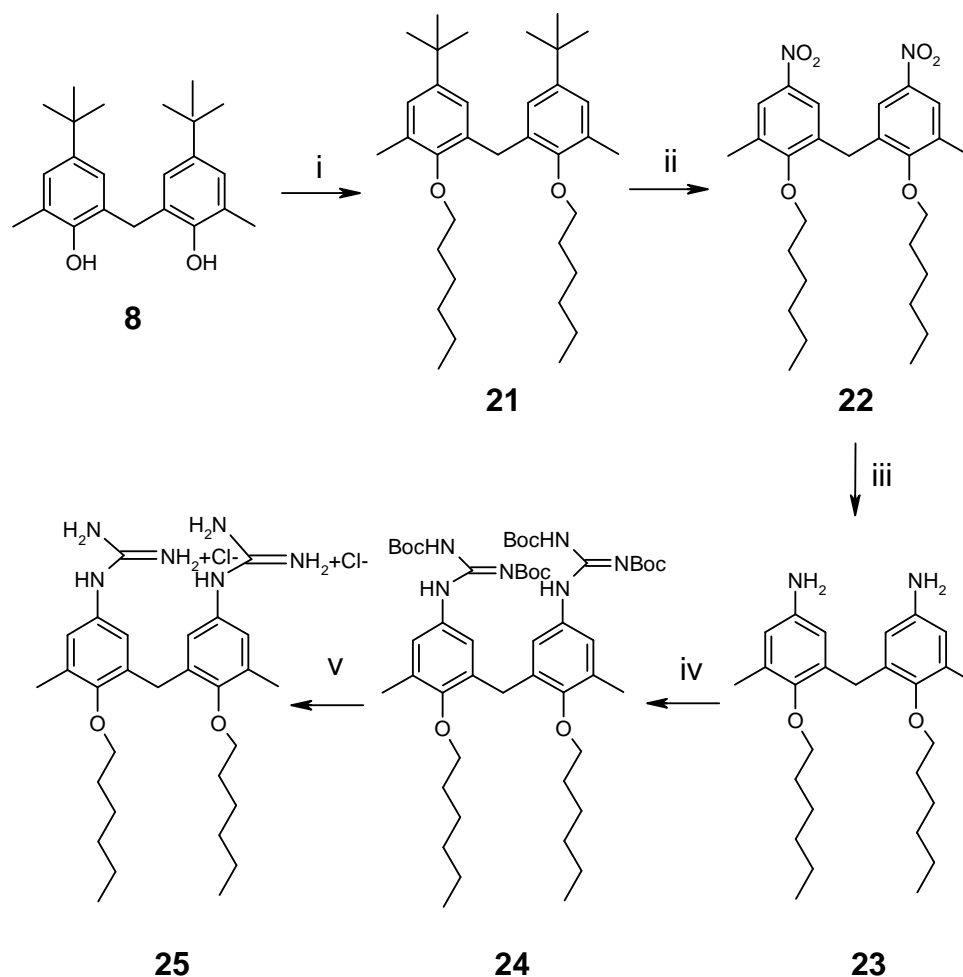


Fig. 2.11. Two views of the energy-minimized structure of Gemini **20b**.

2.2.2.2 Synthesis of the upper rim Gemini analogue

Meanwhile, one Gemini at the upper rim was synthesized, to compare its properties with the lower rim Gemini-type compounds and with its upper rim guanidinium calix[4]arene analogue.²



Scheme 2.5. Synthesis of Gemini **25**. i) HexI, NaH, dry DMF, N₂, rt; ii) NaNO₃, TFA, rt; iii) NH₂NH₂·H₂O, Pd/C (10%), abs EtOH, N₂, reflux; iv) N,N'-di-Boc-N"-triflylguanidine, Et₃N, dry CH₂Cl₂, N₂, rt; v) HCl 37%, 1,4-dioxane, rt.

The synthesis is similar to that of the previously reported upper rim calixarene analogue⁹ and involves the transformation of 2,2'-diphenylmethane derivative **8** into its corresponding O-alkylated derivative **21** by reaction with an excess of iodo-hexane and NaH in dry DMF. Ipsonitration by NaNO₃ in CF₃COOH gave the nitro derivative **22** in acceptable yields. Two by-products **26** and **27** (**Fig. 2.12**) were isolated and characterized from the crude reaction mixture, indicating an unusual reactivity of the substrate during ipsonitration, which was not

previously observed with calixarenes. Subsequent reduction of **22** using $\text{NH}_2\text{NH}_2\cdot\text{H}_2\text{O}$ and a catalytic amount of Pd/C (10%) in refluxing absolute ethanol led to the amino derivative **23**. The final guanidinium product was formed by the same reaction used for lower rim calix[4]arene, with N,N'-di-Boc-N''-triflylguanidine, but in presence of Et_3N , yielding the protected guanidine **24**; cleavage of the protective groups using HCl 37% in 1,4-dioxane gave the final product **25**.

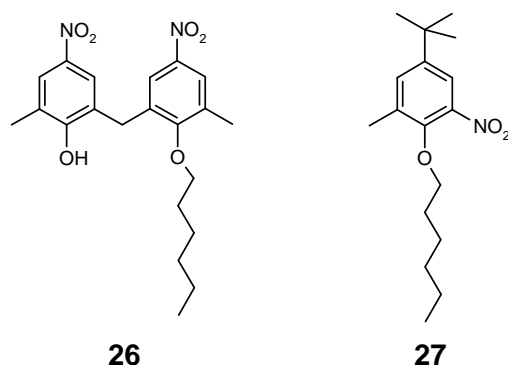


Fig. 2.12. By-products isolated from the ipso-nitration reaction on compound **21**.

All the Gemini-type guanidinium derivatives **20a-c** and **25** resulted soluble in water. ^1H NMR spectra in D_2O at room temperature show sharp signals (**20a** at least until 1 mM, **Fig. 2.13**, **20b** at least until 80 mM, **Fig. 2.14**). The two Gemini **20c** and **25** with longer alkyl chains gave rise, on the contrary, to spectra with broad signals. These became sharp going down to 60 and 500 μM for **20c** (**Fig. 2.15**) and **25** (**Fig. 2.16**), respectively, revealing extended aggregation phenomena due to the larger apolar moieties of this compounds. So, once again at the lower concentration (10^{-5} M) used in the biological studies, no aggregation was observed for all the investigated compounds.

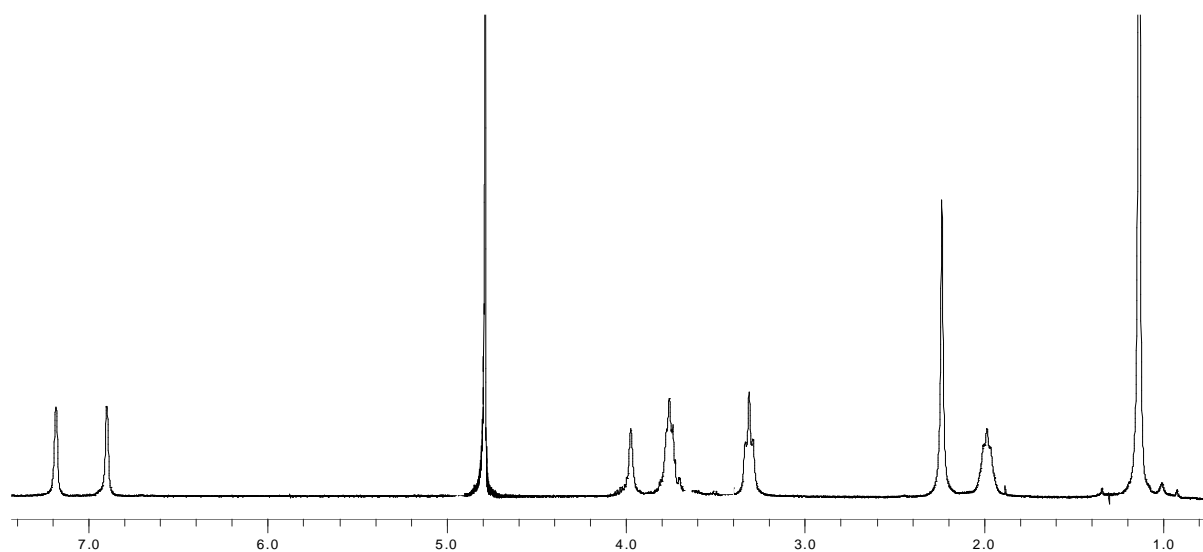


Fig. 2.13. ^1H NMR spectrum (D_2O , 300 MHz, 293 K) of **20a**, 1 mM.

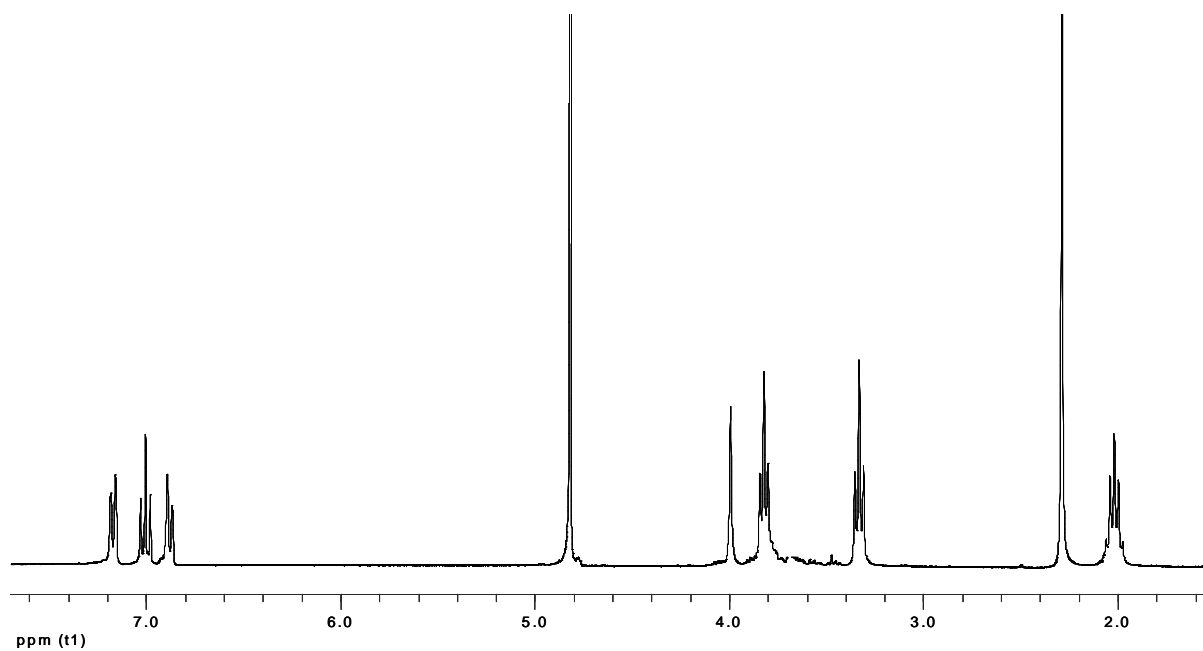


Fig. 2.14. ^1H NMR spectrum (D_2O , 300 MHz, 293 K) of **20b**, 80 mM

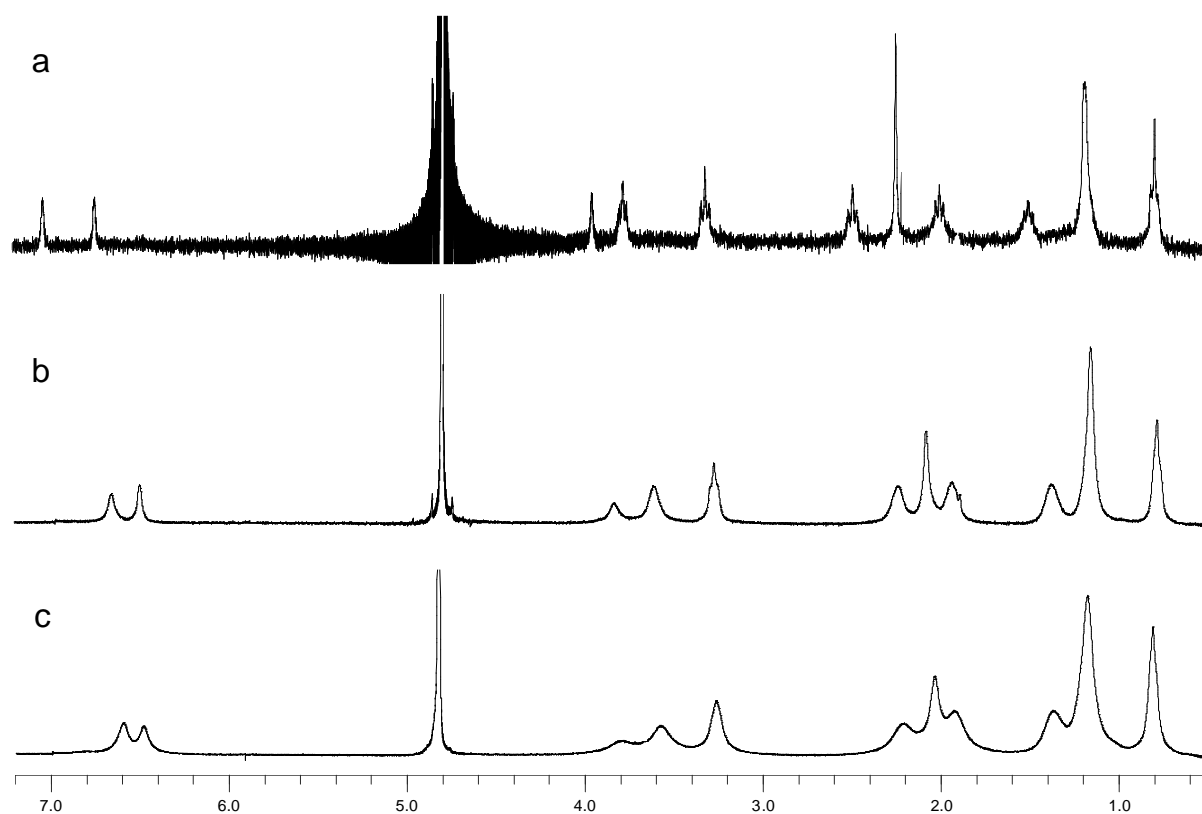


Fig. 2.15. ^1H NMR spectra (D_2O , 300 MHz, 293 K) of **20c**. a) 60 μM , b) 1 mM, c) 40 mM.

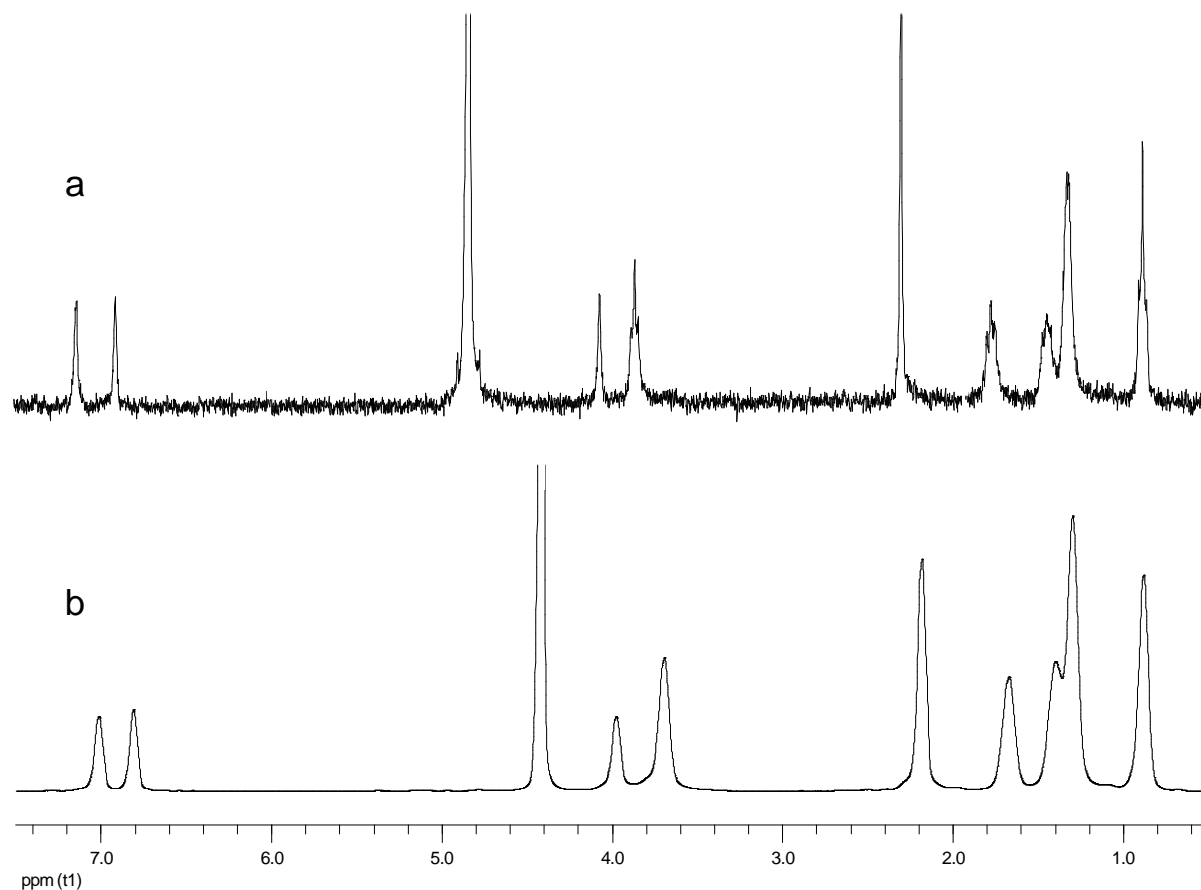


Fig. 2.16. ^1H NMR spectra of **25** at a) 500 μM (D_2O , 300 MHz, 293 K) and b) 50 mM (D_2O , 300 MHz, 363 K).

2.2.3 DNA binding

The compounds obtained were preliminarily studied with different techniques to verify their ability to interact with DNA, creating structures called lipoplexes. All the experiments were performed using the pEGFP-C1 plasmid DNA (4731 bp), which expresses for the Enhanced Green Fluorescent Protein. The ability of compounds **5a-c**, **20a-c** and **25** to bind plasmid pEGFP-C1 DNA was initially assessed through gel electrophoresis and ethidium bromide displacement assays. Among Gemini, **20b** and **25** were studied deeply, whereas for the other Gemini compounds only transfection data were collected (see ahead). The electrophoretic data revealed that the DNA mobility is strongly affected by the macrocyclic compounds **5a-c** already at 50 μM (**Fig. 2.17**). The plasmids remain in the well and are not visible in the gel because probably they are in highly condensed aggregates and the staining reagent (ethidium bromide) can not penetrate them. Macrocycle **5b** showed a slightly stronger affinity since at this concentration no evidence at all of DNA is present in the gel, while a certain amount of plasmids is visible free for **5a** and **5c**. Nevertheless, all the three calixarenes are clearly much more efficient than the Gemini analogues. As reported, for example in **Fig. 2.17**, the non

macrocyclic ligand **20b** is not able to affect the run of plasmids even at 200 μM . It is also significant to notice that the efficiency of these lower rim guanidinium calix[4]arenes is higher than that observed, always by EMSA, for the upper rim analogues, previously described.²

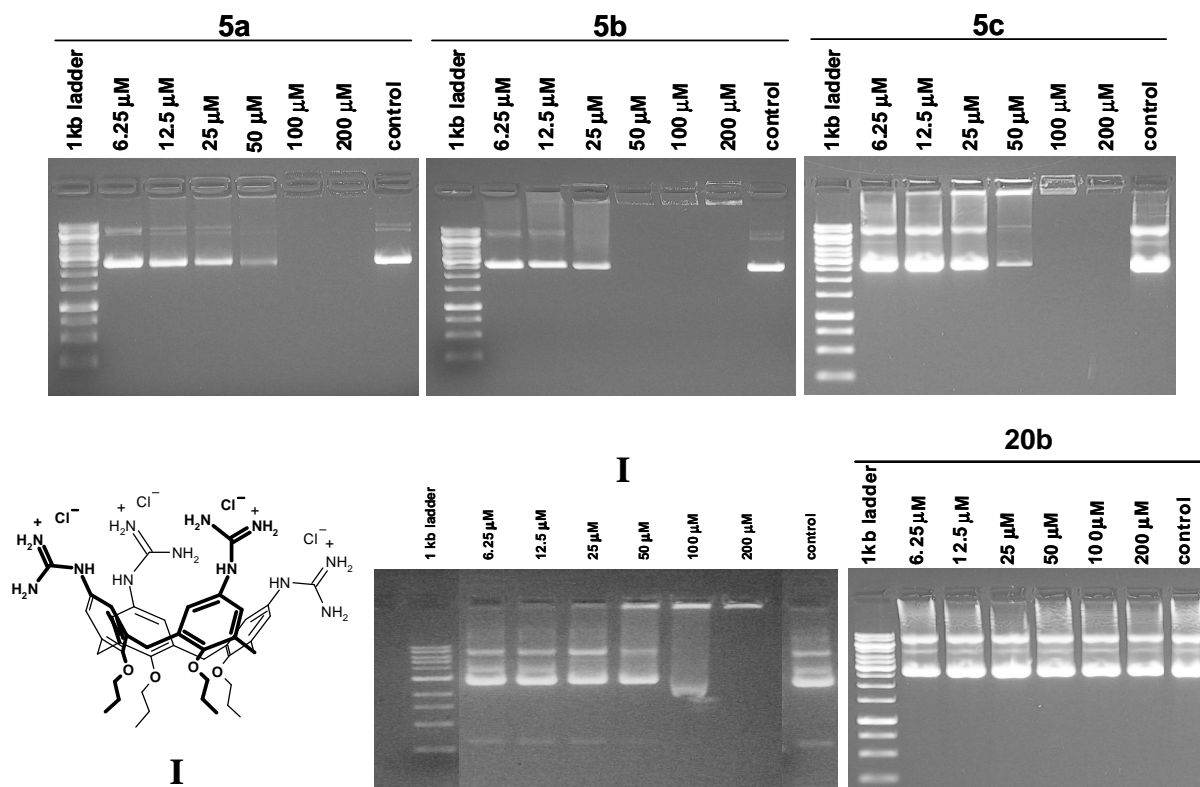


Fig. 2.17. Electrophoresis mobility shift assays performed with plasmid DNA (pEGFP-C1) (25 nM) incubated with guanidinium calix[4]arenes **5a-c** and Gemini **20b**, at increasing concentration (indicated above the gel). The control is the plasmid without ligand.

A second set of experiments was based on Ethidium Bromide Displacement Assay. Ethidium bromide (EtBr) intercalates between the base-pairs of the double helix of the DNA. When intercalation occurs its fluorescence yield, and as a consequence, the fluorescence intensity of the DNA-EtBr complex, increases. If the ligand binds DNA causing displacement of the EtBr, the fluorescence decreases. The relative fluorescence at 600 nm (λ max), defined as the ratio between the fluorescence of the complex EtBr-DNA in presence of ligand and the fluorescence of the complex EtBr-DNA, gives an indication of the interaction strength between the ligand and the DNA. These experiments were conducted titrating a 0.5 nM solution of the DNA-EtBr complex with a 1 mM solution of ligand. The spectrofluorimetric titration showed an evident interaction between calixarenes and the DNA (**Fig. 2.18**). The first additions of **5a-c** to the ethidium bromide/DNA mixture resulted in a drastic and regular fluorescence quenching. However, at higher ligand concentrations (at N/P ratio of 4.2 for **5a**,

8.5 for **5b**, and 5 for **5c**, N/P = guanidinium/phosphate ratio), a marked change in the slope of the titration curve occurred. This is probably due to interactions between ethidium bromide and DNA-calixarene complex, which prevent a quantitative evaluation of the ligand affinity for the plasmid.

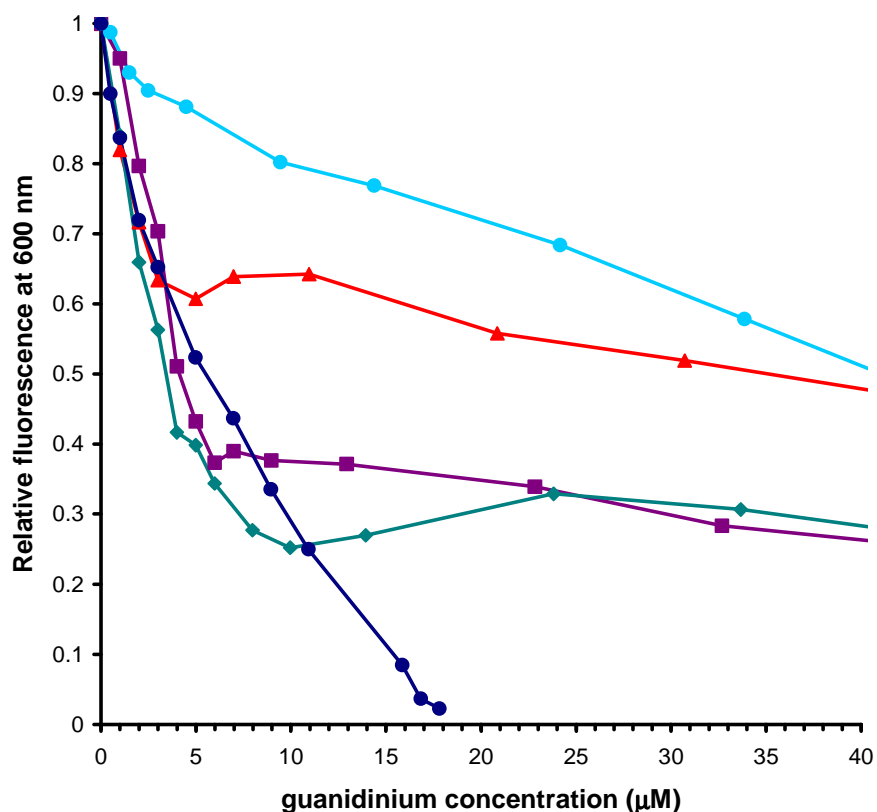


Fig. 2.18. Ethidium Bromide Displacement Assays. Relative fluorescence vs guanidinium concentration. Fluorescence studies (excitation at 530 nm, emission at 600 nm) were performed collecting the emission spectra of buffer solutions (4 mM Hepes, 10 mM NaCl) of 50 mM ethidium bromide (relative fluorescence = 0), mixture of 0.5 nM plasmid DNA (pEGFP-C1) and 50 mM ethidium bromide (relative fluorescence = 1) and after addition of increasing amounts of guanidinium ligand to the DNA/ethidium bromide mixture. A steep decrease in relative fluorescence indicates high efficiency in ethidium bromide displacement and, consequently, in the DNA binding. Light blue line: **20b**, red line: **5a**, violet line: **5c**, green line: **5b**, blue line: **25**.

Completely different is the efficiency in Ethidium Bromide displacement between the two Gemini **20b** and **25**. In fact, while the former binds DNA much less efficiently compared to the guanidinium lower rim calix[4]arenes **5a-c**, at least at guanidinium concentrations below 35 µM, the latter, with the guanidinium groups at the “upper rim” and bearing lipophilic tails, originates a fluorescence quenching very close to that caused by the macrocycles. Moreover, Gemini **25** determines a complete quenching of the fluorescence probably because in this case, differently from **5a-c**, no new interactions between the ligand and the released fluorophores can occur.

In addition to Ethidium Bromide Displacement Assays, the melting curves of pEGFP-C1 DNA plasmid in the linearized form were registered by UV-VIS spectroscopy, in absence and in presence of some of our ligands (**Fig. 2.19**) in order to understand if they stabilize or not the double helix in the binding process.

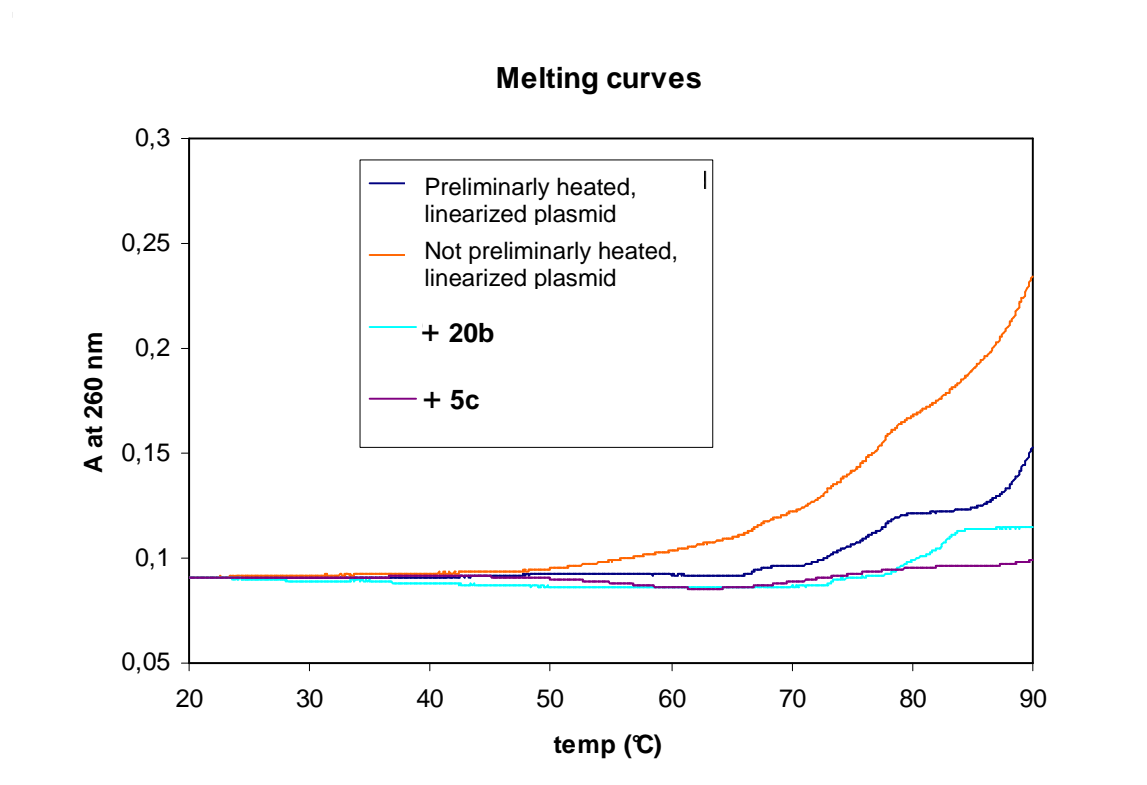


Fig. 2.19. Melting curves of the plasmid DNA previously heated (blue), plasmid DNA not heated (orange), plasmid DNA in presence of Gemini **20b** (light blue) and plasmid DNA in presence of calix[4]arene **5c** (violet).

The melting curves, obtained following Absorbance at a certain λ in function of the temperature T, give in the case of very short oligonucleotides the melting temperature, a parameter which describes the stability of the double helix studied, representing the temperature value where 50% of the helix is denatured. This value was not determined in our case since a long filament was used and, consequently, more than a single melting temperature is present.¹⁰ The melting curves registered in the presence of our ligands were compared with those relative to the DNA alone. As reported for calixarene **5c** and Gemini **20a-c** (**Fig. 2.19**) both type of ligands stabilize the double helix, even if, once again, the macrocyclic compound seems more efficient than the linear one.

Very interesting information on the DNA binding properties of our ligands was obtained by atomic force microscopy (AFM), a technique already successfully used to study the interaction between different synthetic ligands and DNA.¹¹ The experiments were performed with the circular plasmid pEGFP-C1 DNA in tapping mode on air. First, the images were

recorded depositing the DNA onto mica in absence of ligand (**Fig. 2.20a**) and using a buffer rich of Mg^{2+} ions necessary for retaining the filaments on the surface. The filaments appear in the so called relaxed form. There is some overlapping along the simple plasmids but their circular structure can be easily distinguished. Then, images were collected relative to mixtures of the DNA with our ligands after 5 min of incubation (**Fig. 2.20b-d**). In this way the interaction calixarene-DNA and how it affects the plasmid folding were immediately visualized.

A rather intriguing and subtle dependence of the DNA condensation ability of compounds **5a-c** on the alkyl substituent at the upper rim was observed. The p-tert-butyl derivative **5a** forms highly condensed, nanometric aggregates of single DNA plectomenes even at 0.6 μM concentration (**Fig. 2.20b**) with N/P = 0.5, whereas the hexyl derivative **5c** condenses DNA at a concentration of 2.5 μM (N/P = 2) and forms bigger condensates constituted by different filaments (**Fig. 2.20c**). On the contrary, the upper rim unsubstituted compound **5b** does not form tight condensates, although the single plectomenes are much more constrained (**Fig. 2.20**) with respect to their relaxed state (**Fig. 2.20a**), due to their interaction with the charged guanidinium groups of the ligand. However, at concentrations of **5b** higher than 5 μM (N/P \geq 4), no DNA results deposited on the mica surface. Apparently, in these conditions, **5b** causes the complete masking of the DNA negative charges preventing its deposition, or, alternatively, very big aggregates are formed bringing all the DNA filaments in few regions of the mica surface statistically difficult to be found out. The compact condensates formed by **5a** and **5c** are partially relaxed (**Fig. 2.20e** and **2.20f**, respectively) upon addition of 10% v/v of ethanol in the buffer solution during incubation, while in the case of the para-unsubstituted **5b** at 1.8 μM (N/P = 1.5) the presence of the alcohol favours the plasmid condensation (**Fig. 2.20g**).

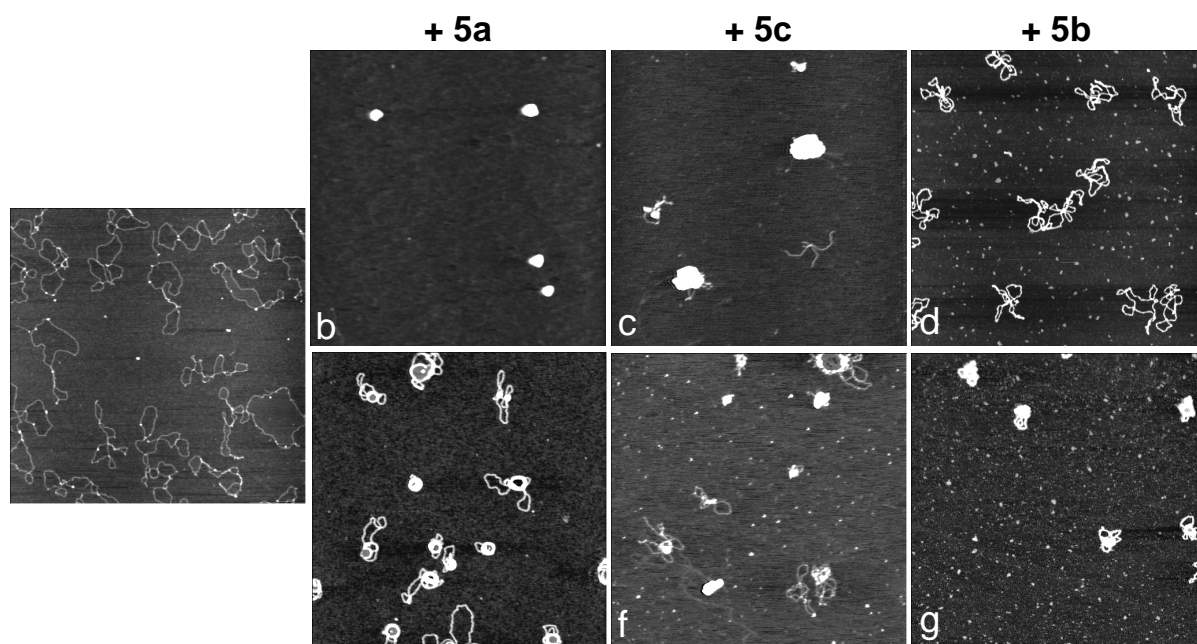


Fig. 2.20. AFM images showing the effects induced on plasmid DNA by guanidinium ligands **5a-c** (upper row) and effects induced by 10% ethanol (v/v) on their condensation activity (lower row). All images were obtained with the microscope operating in tapping mode in air and with supercoiled pEGFP-C1 plasmid deposited onto mica at a concentration of 0.5 nM. (a) Plasmid alone. Plasmid incubated with (b) **5a** 0.6 μM ; (c) **5c** 2.5 μM ; (d) **5b** 1.8 μM ; (e) **5a** 0.6 μM + 10% EtOH; (f) **5c** 2.5 μM + 10% EtOH; (g) **5b** 1.8 μM + 10% EtOH. Each image represents a $2 \times 2 \mu\text{m}$ scan.

Performing the same experiments on Gemini-type ligands, no DNA condensation at all was observed with **20b** (up to 50 μM , N/P = 20) with or without ethanol, although the interaction between our compound and DNA is clear, as shown by the constrains observed in the plectomenes deposited on the mica (**Fig. 2.21i**). The other two “lower rim” Gemini **20a** (**Fig. 2.21a-d**), and **20c** (**Fig. 2.21e-g**), and the “upper rim” Gemini **25** (**Fig. 2.21h-j**), which have a bigger aliphatic region, at a concentration of 2-10 μM and in presence of EtOH, are able to condense the DNA in small mono-filament condensates, even if increasing amount of alcohol from 5 to 10% the process seems to be favoured for **20a** and disfavoured for **20c** and **25**. Moreover, it can be noticed as a particular behaviour that the Gemini **20a** at 5 μM + 5% EtOH gives toroidal condensates (**Fig. 2.21c**).¹²

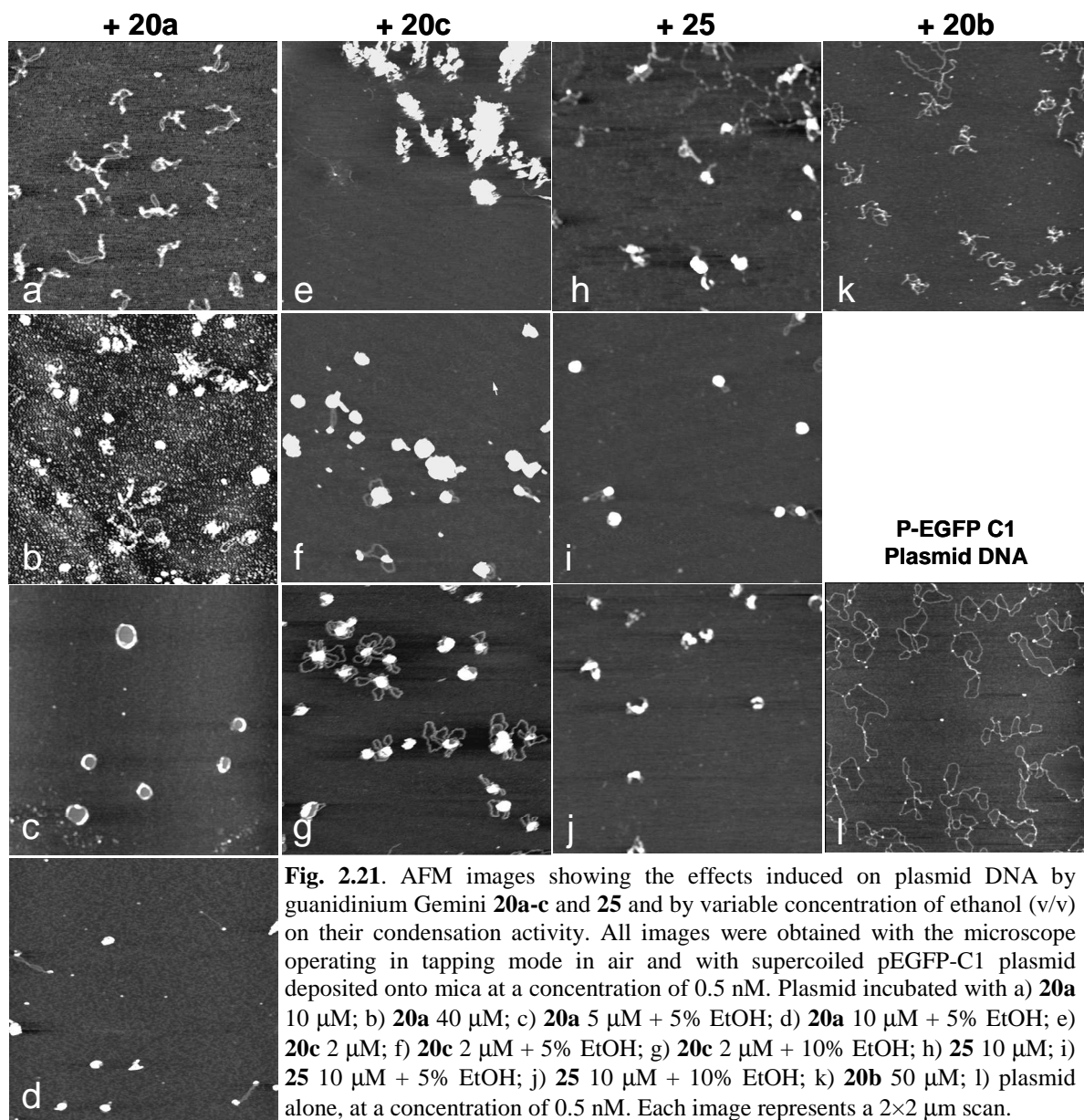


Fig. 2.21. AFM images showing the effects induced on plasmid DNA by guanidinium Gemini **20a-c** and **25** and by variable concentration of ethanol (v/v) on their condensation activity. All images were obtained with the microscope operating in tapping mode in air and with supercoiled pEGFP-C1 plasmid deposited onto mica at a concentration of 0.5 nM. Plasmid incubated with a) **20a** 10 μ M; b) **20a** 40 μ M; c) **20a** 5 μ M + 5% EtOH; d) **20a** 10 μ M + 5% EtOH; e) **20c** 2 μ M; f) **20c** 2 μ M + 5% EtOH; g) **20c** 2 μ M + 10% EtOH; h) **25** 10 μ M; i) **25** 10 μ M + 5% EtOH; j) **25** 10 μ M + 10% EtOH; k) **20b** 50 μ M; l) plasmid alone, at a concentration of 0.5 nM. Each image represents a $2 \times 2 \mu$ m scan.

2.2.4 Transfection properties

Encouraged by the biophysical evidence of DNA binding and condensation, transfection experiments were performed on RD-4 human rhabdomyosarcoma cells using plasmid pEGFP-C1 DNA (1 nM) which, as previously said, expresses a green fluorescent protein easily detectable in the cell by fluorescence microscopy. This cell line was chosen because, beyond the medical relevance, it is easy to grow and not very easily transfectable by traditional methods especially if compared to other cell lines, more widely such as HEK 293 cells and therefore they are useful to test the real transfection capability of the studied compounds. Transfection and cytotoxicity studies were performed by Prof. Gaetano Donofrio at the

Department of Animal Health at the University of Parma. A first important data is that no transfection occurs when either DOPE (**Fig. 2.22**) or ligands **5a-c** are used alone.

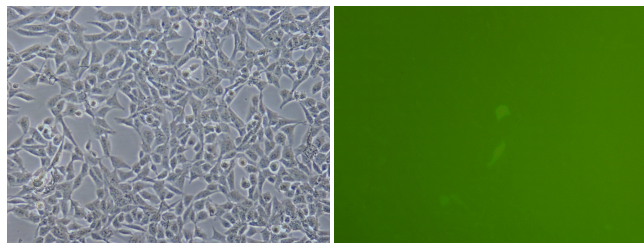


Fig. 2.22. Transfection experiments performed to RD-4 human rhabdomyosarcoma cells with DOPE (20 μM) alone. Cells are visualized with fluorescence microscopy (right column, cells in light green if they express the enhanced green fluorescence protein EGFP) and phase contrast microscopy (left column).

On the contrary, the formulation ligand/DOPE (1/2 molar ratio) especially at ligand 10 μM (N/P = 4) is quite effective. In these conditions (**Fig. 2.23**), in particular compound **5b** is a very efficient transfectant for RD-4 human rhabdomyosarcoma cells.

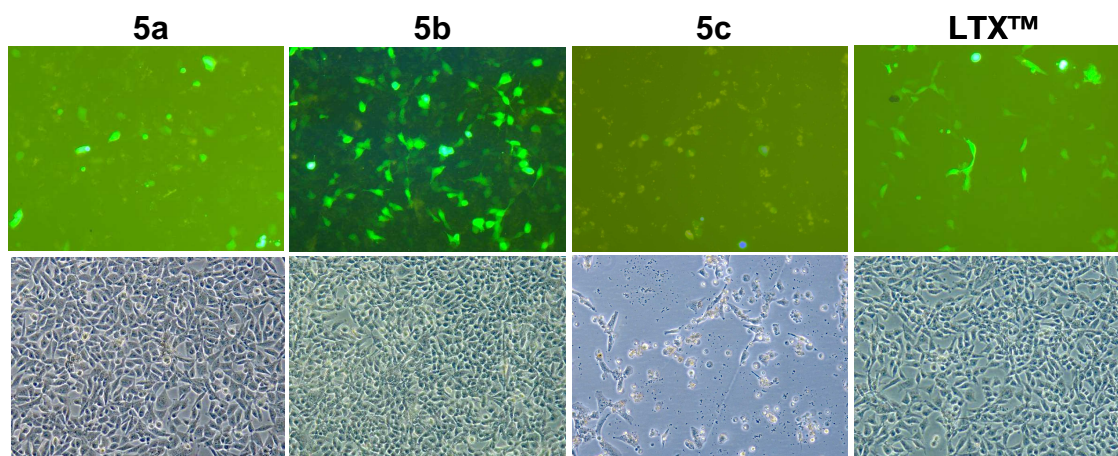


Fig. 2.23. Transfection experiments performed with pEGFP-C1 plasmid 1 nM, guanidinium calixarene **5a-c**/DOPE (1/2 molar ratio, 10/20 μM), and lipofectamine LTX[™] formulations to rhabdomyosarcoma cells. Transfected cells are visualized with fluorescence microscopy (upper row, in light green because they express the enhanced green fluorescence protein EGFP) and phase contrast microscopy (lower row).

Remarkably, (**Fig. 2.23** and **2.24**) the amount of transfected cells for **5b** (48%) is higher than that achieved by the commercially available lipofectamine LTX[™] 12 (30%) containing DOPE and by the previously investigated upper rim tetraguanidinium calix[4]arenes (less than 20%). Moreover, little transfection activity is observed for compounds **5a** (3-4%, **Fig. 2.23**) and **5c** (6-7%, **Fig. 2.23**).

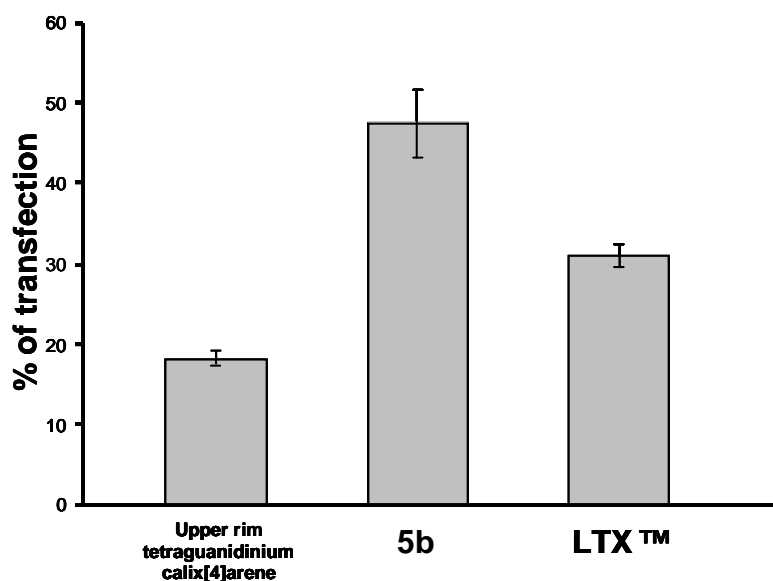


Fig. 2.24. In vitro transfection efficiency as percentage of transfected cells observed upon treatment of RD-4 human rhabdomyosarcoma cells with guanidinium derivative/DOPE formulations and lipofectamine LTX™.

Quite rewarding was also the finding that the most active compound **5b** has a very low cytotoxicity (**Fig. 2.25**) showing 75-80% of cell viability at 48 h from transfection. Similar results were obtained with **5a**, while **5c** is more toxic (60% of cell viability).

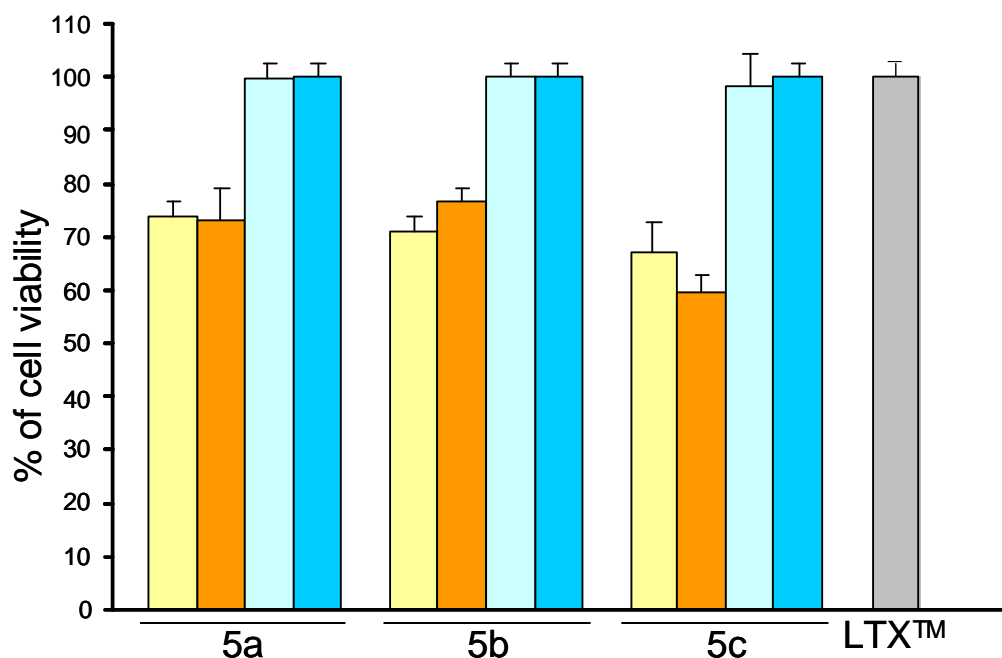


Fig. 2.25. Post-transfection cell viability in the presence of ligand alone (yellow bars), ligand/DOPE (10 μM/20 μM) formulation (orange bars), DOPE alone (light blue bars), without any treatment (blue bars), and in the presence of LTX™ (grey bar).

All the “alkyl” Gemini **20a**, **20c**, **25** resulted quite toxic and probably for this reason with a very low transfection efficiency (**Fig. 2.26**). They were incubated at a double concentration with respect to the calixarene derivatives, to have the same N/P ratio. Only **20b** (ca. 6% at 20 μM) and **25** (ca. 14% at 20 μM) resulted slightly efficient (**Fig. 2.27**).

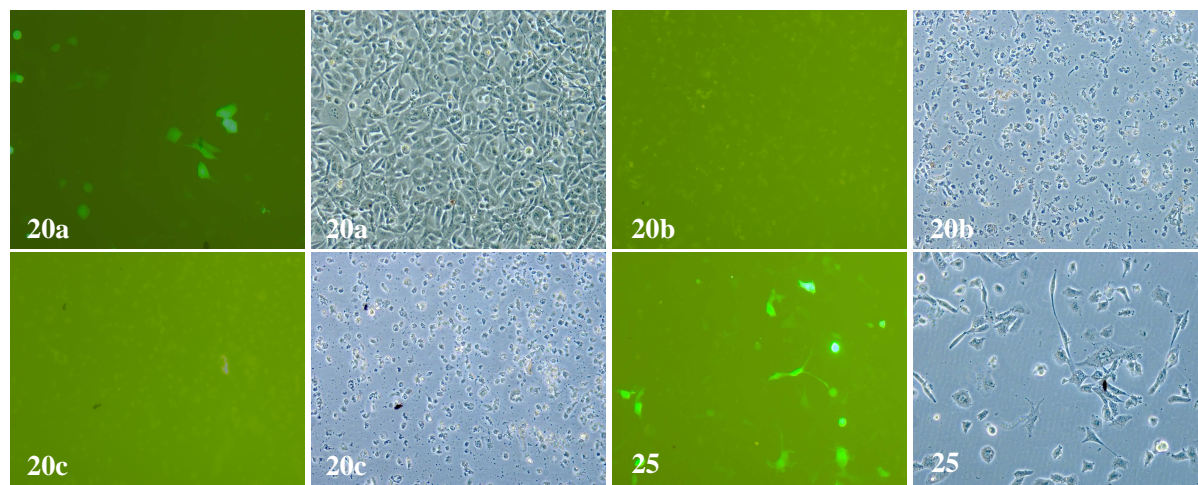


Fig. 2.26. Transfection experiments performed with guanidinium Gemini **20a**, **20b**, **20c**, **25** (20 μM) and DOPE (40 μM) to RD-4 human rhabdomyosarcoma cells. Cells are visualized with fluorescence microscopy (first and third columns, cells in light green if they express the enhanced green fluorescence protein EGFP) and phase contrast microscopy (second and fourth columns).

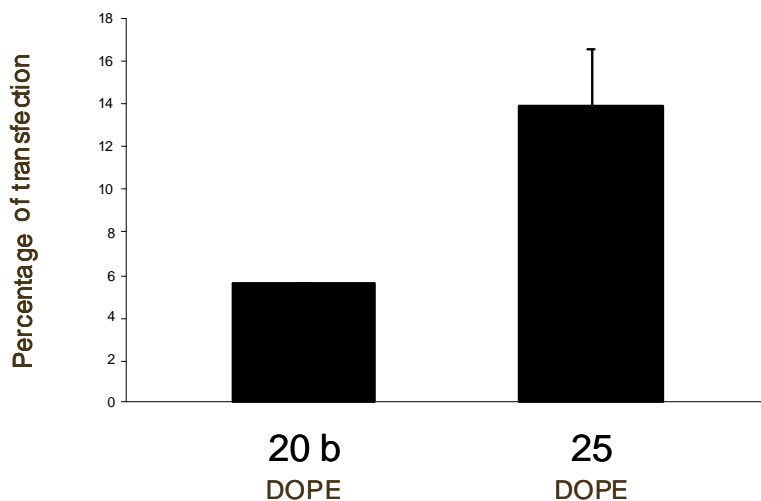


Fig. 2.27. In vitro transfection efficiency as percentage of transfected cells observed upon treatment of RD-4 human rhabdomyosarcoma cells with guanidinium Gemini derivative/DOPE formulations.

Since it is well-known in the field of synthetic nonviral vectors that transfection efficiency may depend on the type of cell used, our lead compound **5b** was tested in a varying cell line setting using again LTXTM as a reference (**Fig. 2.28**). Comparable results between the two formulations were obtained with AUBEK and BoMAK cells, whereas LTXTM is definitely more active in the case of hMSC and N2a cell lines. The reverse is true for Vero cells which

are not transfected at all by the commercial product LTXTM, while **5b**/DOPE gives transfection (ca. 12%).

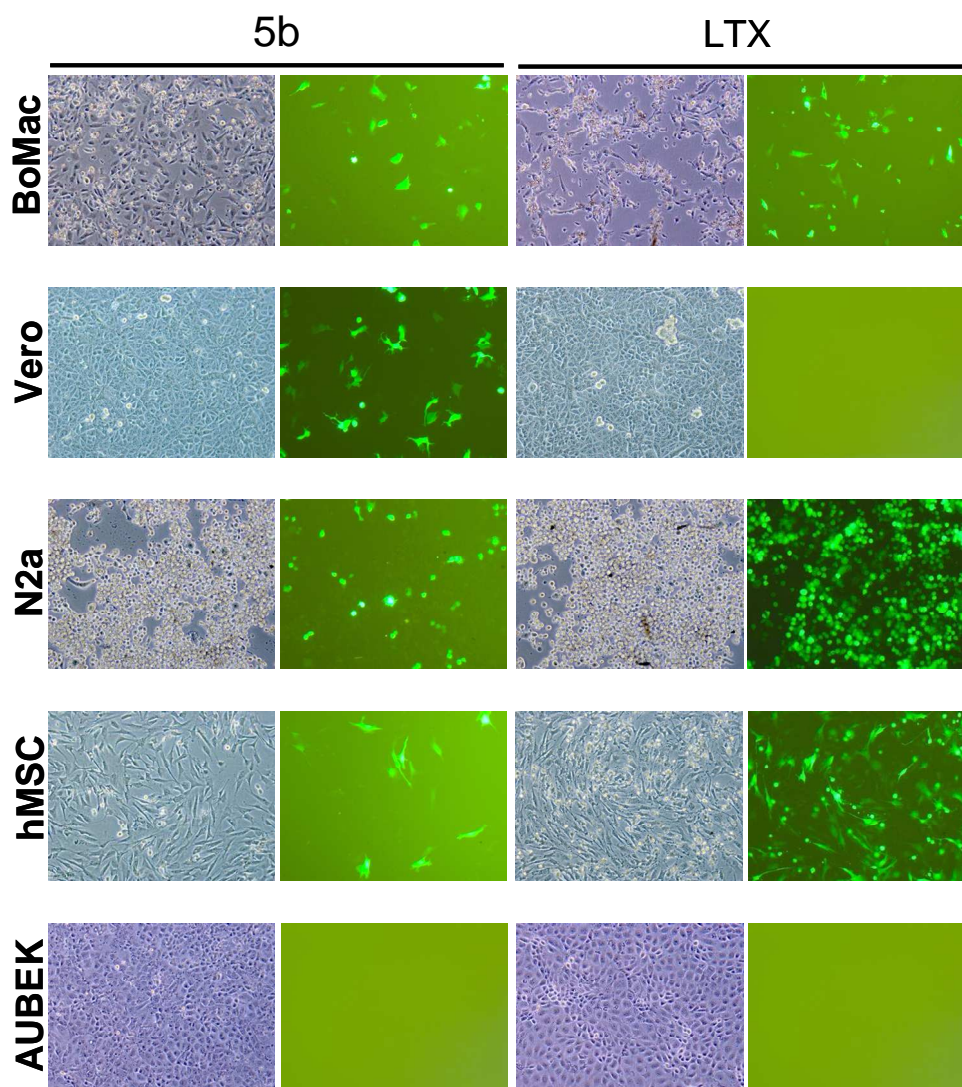


Fig. 2.28. Transfection experiments performed with **5b**/DOPE (1:2 molar ratio, 10/20 μ M) formulation and LTXTM using different cell lines. Transfected cells are visualized with fluorescence microscopy (2nd and 4th columns, in light green because they express the enhanced green fluorescence protein EGFP) and phase contrast microscopy (1st and 3rd columns).

2.3 Conclusions

Comparison of the DNA condensation and cell transfection efficiency of the most active compound **5b** with its open chain analogue **20b**, having a very similar lipophilic/hydrophilic ratio, suggests a possible positive role of the macrocyclic scaffold on gene delivery to cell.

In general the linear Gemini analogues in view of their low efficiency and, for the most apolar character, of the high cytotoxicity, are not useful in terms of transfection.

From the AFM studies it was deduced that in the para-alkyl substituted macrocycles **5a** and **5c** the primary electrostatic interaction between the guanidinium groups and the DNA phosphate anions is followed by hydrophobic interactions between the alkyl chains at the upper rim. The latter interactions, which induce the formation of condensates, are partially lost in hydroalcoholic solution. On the contrary, in the case of **5b**, which lacks alkyl chains at the upper rim, only charge-charge interactions, which are strengthened in the ethanol/water mixture, control the DNA condensation process. Overall, the former “double interaction” mechanism in DNA condensation is more efficient than the latter “single interaction” pathway, and this explains the AFM results.

It is not surprising that it was not found a strict correlation between the transfection efficiency of the **5a-c**/DOPE formulations and the ability of the ligands to condense DNA as disclosed by AFM studies. In fact, cell transfection achieved with cytofectin/DOPE formulations is a complex supramolecular function, and many important steps outside and inside the cell must be positively affected to get the goal.¹⁴

Some hypotheses can be put forward to explain in particular the better performance of the lower rim guanidinium calix[4]arene **5b** as non viral vector compared to its upper rim analogue. One is the presence of guanidinium groups which could have quite different pKa values. In particular, not all the guanidinium groups directly linked to the aromatic ring could be necessarily more protonated since they could be more acid due to resonance effects and to the close proximity one to the other. If true, the alkylguanidinium derivative **5b** would have an higher number of cationic units for the interaction with the negatively charges of the phosphates in the DNA double helix. A second reason could be the flexibility of the chains bearing the guanidinium group in **5b** which would favour it in the binding of DNA and cell membrane phospholipids.¹⁵ The third one could be related to the effect of DOPE on the ligand activity, which is particularly marked in the case of the lower rim ones. For this aspect, the position of charged groups with respect to the calixarene cavity and thus, the availability, especially in **5b**, for interaction with the phospholipid helper thus allowing the formation of peculiar supramolecular assemblies Calixarene-DOPE more suitable for transfection.

Physico-chemical studies on this aspect are currently in progress by Prof. Pietro Baglioni's group at the University of Florence. In summary attaching the guanidinium groups at the phenolic oxygen atoms (lower rim) of calix[4]arenes discloses the possibility to significantly enhance the cell transfection ability of these synthetic cationic lipids formulated with DOPE and reduces their toxicity to cells, if compared to the same macrocycles with the charged

groups directly linked to the aromatic nuclei (upper rim). The DNA binding and condensation properties, cell transfection ability, and toxicity shown by the macrocyclic cytofectins **5a-c** strongly depend on the substituents at the upper rim of the calixarene. Notably, the transfection efficiency of the little toxic **5b**/DOPE formulation is even higher than that of the commercially available LTXTM in the case of RD-4 human rhabdomyosarcoma and Vero cell lines. The results obtained warrant further studies aimed at elucidating the mechanism of cellular uptake and intracellular trafficking of this novel DNA delivery system and its cargo to establish a structure-activity relationship. Some of them are reported in the following chapter, while others are ongoing in the group laboratory.

2.4 CO₂ Capture by Multivalent Amino-functionalized Calixarenes

In the description of the synthetic procedures followed to obtain our vectors **5a-c** and reported above it was mentioned the need to prevent, in particular during the work-up procedure for their isolation, the undesired reaction between the amino intermediates **3a-c** (**Fig. 2.29**) and atmospheric CO₂. Indeed, it was decided to investigate separately and more deeply this behaviour also considering the interest for systems able to capture CO₂ from the environment. There is little doubt, nowadays, that the level of atmospheric CO₂, one of the major greenhouse gases, is dramatically increasing, mainly due to the burning of fossil fuels, to cement manufacturing and to deforestation.¹⁶ Therefore, any system able to trap and sequester CO₂ from the environment or any process that utilizes CO₂ as a substrate or a reactant are of great importance.

Tetraamine **3a**, substituted at the upper rim with four t-butyl groups, showed, despite its good degree of purity, a ¹H NMR spectrum, recorded immediately after its synthesis, that revealed the presence of small peaks, corresponding to another species. Compound **3c**, substituted at the upper rim with four n-hexyl groups, even more so, had a ¹H NMR spectrum containing a two patterns of signals relative to **3c** and a second species in ~1:1 ratio (data not shown).

Starting from the hypothesis that interactions with CO₂ was the basis of this experimental evidence, the gas was bubbled through a solution of each compound **3a-c** in a deuterated solvent for 10 min. After this time, the products of the reaction were studied by ¹H NMR, ¹³C NMR and 2D NMR, in particular in the case of tetramino derivative **3b**, confirming the hypothesis done.

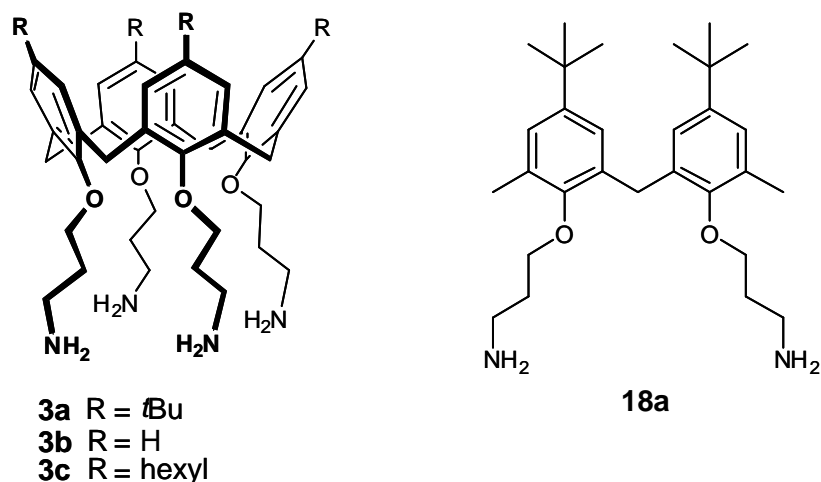
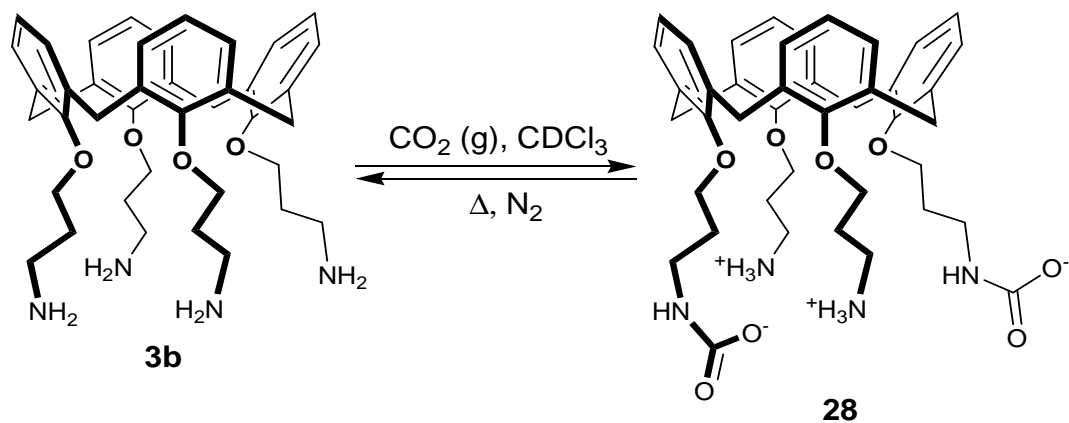


Fig. 2.29. Structural formula of amino calix[4]arenes **3a**, **3b**, **3c** and of diamino derivative **18a**.

In the presence of dissolved CO_2 , the ^1H NMR spectrum of tetraaminocalixarene **3b** in CDCl_3 appears in fact significantly transformed (**Fig. 2.30b**). All the signals belonging to **3b** (**Fig. 2.30a**), disappear, replaced by a new set of resonances which reflect a species of C_2 symmetry compatible with compound **28**, having two ammonium cations and two carbamate anions in alternate positions instead of the four amine groups (**Scheme 2.6**).



Scheme 2.6. Reaction of **3b** with $\text{CO}_2(\text{g})$ in CDCl_3 , to give **28**.

The NH carbamate signal emerges as a triplet at 4.74 ppm, while the NH_3^+ group resonates as a slightly broad signal at 9.35 ppm. Six signals (two of which are superimposed at 3.65 ppm) for the methylene groups replace the three present in the spectrum of **3b**, and are fully assigned on the basis of a COSY spectrum through the cross-peaks between the NH carbamate proton and the NH_3^+ protons and the respective α -methylene protons. In the ^{13}C NMR spectrum the $\text{C}=\text{O}$ signal of the carbamate group appeared at 163.6 ppm and the signal

of the dissolved free CO₂ at 124.7 ppm. Two sets of signals are present for the two different aromatic units and chains. In particular, the single signal of the α carbon is shifted and splitted from 39.5 ppm in **3b** to 41.1 and 36.4 for the carbamate and the ammonium group, respectively. No precipitate is observed in the solution after CO₂ exposure, ruling out the formation of insoluble supramolecular polymers.¹⁷ The spectrum does not change by dilution and also DOSY experiments confirmed the unimolecular nature (data not shown) of the adduct.

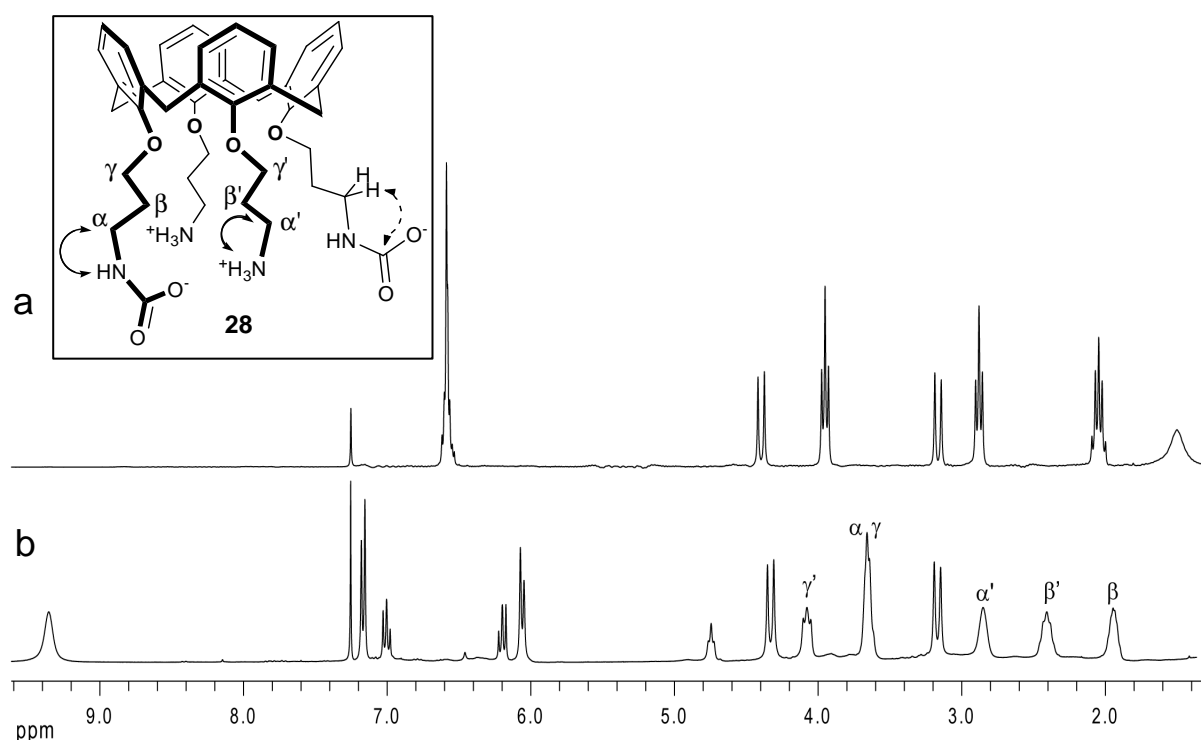
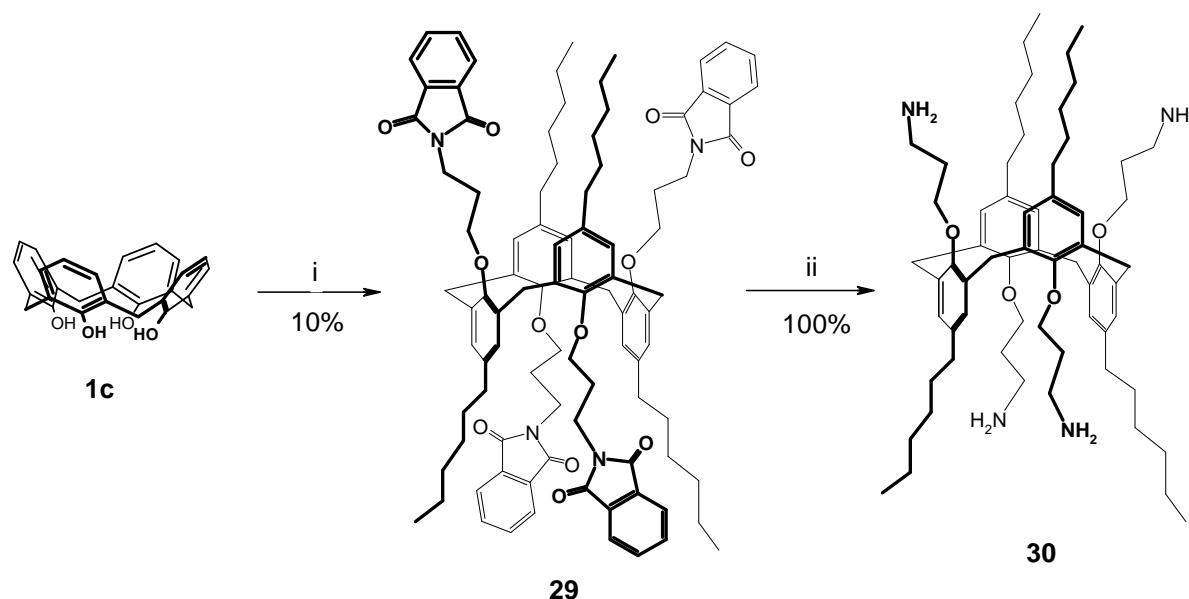


Fig. 2.30. ¹H NMR spectra (300 MHz, CDCl₃, 298 K) of **3b** (a) and **3b** after saturation of the solution with CO₂ (b) with formation of **28**. Inset: curved arrows = COSY cross-peaks; dashed curved arrow = HMBC cross-peak.

The aromatic protons, which in **3b** are isochronous, resonate for **28** in two systems separated by ca 1 ppm (**Fig. 2.30b**). Two reasons can in principle be attributed to this splitting: the presence of the two different substituents at the lower rim, or a flattened cone conformation of the calixarene.¹⁸ The latter possibility is the correct one, since in the ¹H NMR spectrum (see below, **Fig. 2.31**) of the CO₂ adduct of the non-cyclic model compound **18a** (**Scheme 2.8**) the signals of the aromatic protons are not shifted. The conclusion is then that calixarene scaffold adopts a flattened cone conformation and molecular modelling predicts that the aromatic groups linked to the carbamate-terminating chains are pointing inwards, while the four charged groups are connected by a circular array of hydrogen bonds. Both ammonium groups

are involved in two hydrogen bonds, whereas the COO^- anions participate in the network with either a monodentated or a bifurcated hydrogen bond. This pattern of strong hydrogen bonds explains the high stability and inertness of adduct **28**. In fact, once formed, the adduct **28** is highly stable both in solution and at the solid state. The ^1H NMR spectrum of a sample of **28** stored at room temperature remains unchanged for a few weeks and no modifications are observed in the temperature range $-45\div 50$ °C. The release of CO_2 can be achieved only upon heating a solution at 60 °C while flowing N_2 . Alternatively, the acidification of the solution of **28** with HCl results in the disruption of the adduct and the formation of the tetra-ammonium cation of **3b**. Compound **28** can be obtained also washing a dichloromethane or chloroform solution of **3b** with a saturated solution of NaHCO_3 . Treating the separated organic phase with Na_2SO_4 , evaporating the solvent and drying the solid residue *in vacuo* does not affect the product. Moreover, CO_2 absorption from the laboratory air is observed for **3b** in the solid state. Also calix[4]arenes **3a** and **3c** behave in a similar way, so calixarene **30** in the 1,3-alternate conformation analogue of **3c**, was also synthesized, to evaluate the effect of conformational changes on the CO_2 capture ability of the aminocalix[4]arenes.

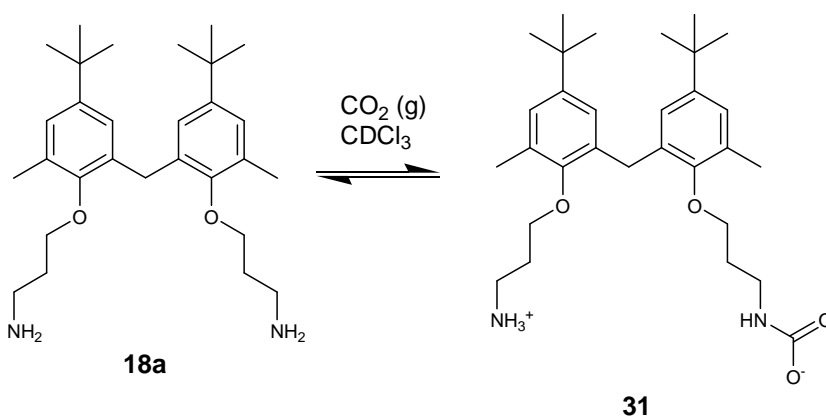
The synthesis of the 1,3-alternate calix[4]arene phthalimides (**Scheme 2.7**) was achieved using Cs_2CO_3 , to block the calix[4]arene in the desired conformation. The yield is quite low because it was difficult to totally functionalized the molecule and because also the cone conformation formed. The removal of the phthalimide group to obtain **30** was again done with $\text{NH}_2\text{NH}_2\cdot\text{H}_2\text{O}$ in the conditions previously used to obtain the other amino derivatives.



Scheme 2.7. Synthesis of compound **30**. i) N-(3-bromopropyl)phthalimide, Cs_2CO_3 , dry THF, N_2 , reflux; ii) $\text{NH}_2\text{NH}_2\cdot\text{H}_2\text{O}$, abs EtOH, N_2 , reflux.

Then CO₂(g) was bubbled into a solution of **30** in CDCl₃, causing a broadening of the ¹H NMR signals, which in this case can be interpreted as due to the formation of a mixture of intramolecular and intermolecular (polymeric) complexes.

The ability in capturing CO₂ was studied also for model compound **18a**. Bubbling CO₂ through a solution of this compound in CDCl₃ resulted in a significant transformation of the ¹H NMR spectrum (**Fig. 2.31**), analogous to that observed for **3b**, and compatible with the formation of an alkylammonium and a carbamate group (**Scheme 2.8**).



Scheme 2.8. Reaction of **18a** with CO₂(g) in CDCl₃.

In particular, two broad signals appeared at 7.93 and 4.88 ppm, assigned to the NH₃⁺ and the carbamate NH, respectively. Six signals for the methylene protons of the alkyl chains replaced the three shown by **18a**. Based on a COSY spectrum, three of these signals were assigned to the alkylammonium chain and the remaining three to the carbamate chain. Two different singlets appeared for the methyl Ar-CH₃ signals, two for the t-butyl signals and four for the ArH protons, two of which are superimposed. In the ¹³C spectrum the C=O carbamate carbon atom resonates at 163.6 ppm.

The stability of the **18a**-CO₂ adduct **31**, however, is significantly lower than that of **28**. After storage of a solution of **31** in a stoppered NMR tube for a few days, the spectrum revealed that CO₂ was slowly released from the adduct and a mixture of **31** and free **18a** are present.

Differently from **28**, in the NOESY and ROESY spectra of **31** chemical exchange peaks are present between the α and α', between the β and β' and between the γ and γ' methylene groups and between the two internal ArH protons, indicating that the CO₂ molecule is exchanging between the ammonium and the carbamate site. Moreover, never observed with amino calix[4]arenes-CO₂ adducts, dilution of a 10 mM sample in CDCl₃ of **31** to 0.1 mM resulted in the disappearance of the signals of the adduct and the presence only of the signals

of the free amine **18a**, confirming the lower stability of this adduct. Washing a chloroform solution of **18a** with NaHCO₃ 0.1 M did not result in the formation of the adduct and no spontaneous absorption of CO₂ from the laboratory air was observed, neither for a solution of **18a** nor for the compound in the solid state. The difference in stability between this adduct and the one based on the calixarene is clearly due to the presence of a lower number of hydrogen bonds between the ammonium and carbamate groups.

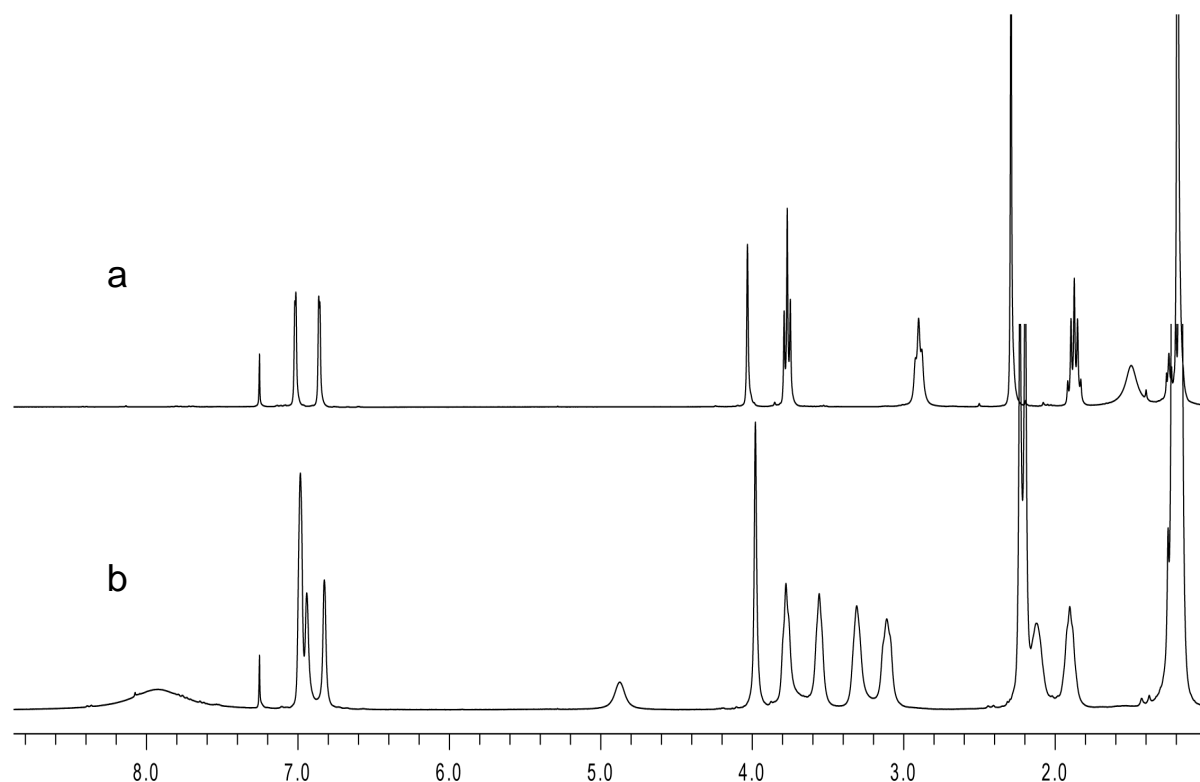


Fig. 2.31. ¹H NMR spectra (300MHz, CDCl₃, 298K) of: a) **18a**; b) after saturation with CO₂, with formation of **31**.

In the presence of CO₂ the aminocalixarenes **3a-c**, **29** and the linear compound **18a** reacted giving carbamates. The spatial proximity of the two ammonium cations and the two carbamate anions in the cone calix[4]arenes allows for the formation of a circular array of strong hydrogen bonds, which explains the high stability and inertness of, for example, adduct calix[4]arene-CO₂ **28** compared to **31**, which derives from the linear compound **18a**. The 1,3 alternate calix[4]arene, in presence of CO₂, originates a mixture of inter and intramolecular hydrogen bonded complexes.

2.5 Experimental section

All the reactions were carried out under a nitrogen atmosphere. All dry solvents were prepared according to standard procedures and stored over molecular sieves. Melting points were determined on an Electrothermal apparatus in capillaries sealed under nitrogen. ^1H and ^{13}C NMR spectra were recorded on Bruker AV300 and AC300 spectrometers (partially deuterated solvents were used as internal standards). Mass spectra were recorded in ESI mode on a single quadrupole instrument SQ Detector, Waters (capillary voltage 3.8 kV, cone voltage 30-160 eV, extractor voltage 3 eV, source block temperature 80 °C, desolvation temperature 150 °C, cone and desolvation gas (N_2) flow rates 1.6 and 8 L/min, respectively). UV and Fluorimetric experiments were performed on Perkin Elmer UV-Vis Lambda BIO 20 spectrophotometer and LS55 Perkin Elmer fluorimeter, respectively. Elemental analyses were performed using a Termoquest 1112 CHN instrument and are reported as percentage. TLC was performed on Merck 60 F254 silica gel and flash column chromatography on 230-240 mesh Merck 60 silica gel.

Synthesis of Hexanoyl Chloride (similar to a procedure in ref. 3).

To a solution of hexanoic acid (15 mL, 119.7 mmol) in dry CH_2Cl_2 (13 mL), $(\text{COCl})_2$ (14 mL, 160.5 mmol) and DMF (8 drops) as catalyst were added and the mixture was stirred for 1 h at room temperature. The product is obtained after the removal of the solvent under reduced pressure as a yellow liquid in 96% yield.

^1H NMR (300 MHz, CDCl_3) δ 2.88 (t, $J = 7.2$ Hz, 2H, COCH_2), 1.72 (quint, $J = 7.3$ Hz, 2H, COCH_2CH_2), 1.37-1.31 (m, 4H, $\text{COCH}_2\text{CH}_2\text{CH}_2\text{CH}_2$), 0.93-0.88 (m, 3H, CH_3).

Synthesis of Bis[(2-hydroxy-3-methyl-5-*tert*-butyl)phenyl]methane (8).

To a suspension of Mg (1.44 g, 60 mmol) in dry THF (60 mL), a solution of EtBr (5.24 mL, 60 mmol) in dry THF (40 mL) was added dropwise. Subsequently, a crystal of I_2 was added and the reaction mixture heated to reflux. When all the Mg was reacted, a solution of 4-*tert*-butyl-2-methylphenol **7** (9.84 g, 60 mmol) in dry THF (60 mL) was added dropwise. After 2 min the solvent was removed under reduced pressure and the remaining solid was dissolved in toluene (200 mL). Paraformaldehyde (0.9 g, 30 mmol) was added to the stirring solution and the reaction mixture was heated at 120 °C. After 6 h the reaction was quenched with 1 N HCl (150 mL), and the water phase extracted with diethyl ether (2×100 mL). The organic layers were combined, dried over anhydrous Na_2SO_4 and concentrated under reduced pressure. The

product was crystallized from hexane to give the pure compound as a white solid in 25% yield. Compound **8** shows the same spectroscopic and physical data reported in the literature.⁶ ¹³C NMR (75 MHz, CDCl₃) δ 148.7, 143.5, 126.1, 125.9, 125.1, 123.3, 33.9, 31.7, 31.5, 16.3.

Synthesis of Bis[(2-hydroxy-3-methyl)phenyl]methane (9).

It was synthesized according to a literature procedure and shows the same spectroscopic and physical properties.⁷

¹³C NMR (75 MHz, CDCl₃) δ 151.0, 129.3, 128.4, 126.2, 123.9, 120.9, 31.0, 15.9. MS (ESI), (negative ion mode): calculated for [M - H]⁻ *m/z* = 227.1, found *m/z* = 227.0.

Synthesis of Bis[(2-hydroxy-3-methyl-5-hexanoyl)phenyl]methane (10).

It was synthesized according to a literature procedure and shows the same spectroscopic and physical properties.⁷

The crude was purified by flash column chromatography on silica gel (eluent: CH₂Cl₂, CH₂Cl₂/MeOH= 98:2) to obtain the pure product **10** as a white solid in 40% yield.

¹³C NMR (75 MHz, CDCl₃) δ 199.5, 155.4, 130.3, 130.0, 129.1, 125.7, 124.0, 38.2, 31.5, 30.9, 24.3, 22.5, 16.0, 13.9. MS (ESI): calculated for [M - H]⁻ *m/z* = 423.3, found *m/z* = 423.2.

Synthesis of 5,11,17,23-Tetra-*n*-hexyl-25,26,27,28-tetrahydrocalix[4]arene (1c).

It was synthesized according to a literature procedure and shows the same spectroscopic and physical properties.⁵

¹³C NMR (75 MHz, CDCl₃) δ 146.6, 136.3, 128.7, 128.0, 35.1, 31.9, 31.7, 31.4, 29.0, 22.6, 14.0. MS (ESI): calculated for [M + Na]⁺ *m/z* = 783.5, found *m/z* = 783.6.

Synthesis of Bis[(2-hydroxy-3-methyl-5-hexyl)phenyl]methane (11). It was synthesized according to a literature procedure for its calix[4]arene analogue.⁶ The crude was purified by flash column chromatography on silica gel (eluent: CH₂Cl₂) to obtain the pure product as a white solid in 79% yield.

Mp: 78-80 °C. ¹H NMR (300 MHz, CDCl₃) δ 6.97 (d, *J* = 1.8 Hz, 2H, ArH), 6.82 (d, *J* = 1.8 Hz, 2H, ArH), 6.22 (bs, 2H, OH), 3.90 (s, 2H, ArCH₂Ar), 2.50 (t, *J* = 7.5 Hz, 4H, ArCH₂), 2.21 (s, 6H, ArCH₃), 1.58 (quint, *J* = 5.9 Hz, 4H, ArCH₂CH₂), 1.40-1.30 (m, 12H, ArCH₂CH₂CH₂CH₂CH₂), 0.92 (t, *J* = 6.5 Hz, 6H, CH₂CH₃). ¹³C NMR (75 MHz, CDCl₃) δ 148.9, 135.3, 129.2, 128.1, 126.2, 123.8, 35.1, 31.7, 31.4, 29.0, 22.6, 16.0, 14.1. MS (ESI): calculated for [M - H]⁻ *m/z* = 395.3, found *m/z* = 395.4.

Synthesis of 5,11,17,23-Tetra-*t*-butyl-25,26,27,28-tetrakis(3-phthalimidopropoxy)calix[4]arene (2a) and 25,26,27,28-tetrakis(3-phthalimidopropoxy)calix[4]arene (2b) were synthesized according to literature procedures.^{6b,6c}

General procedure for the alkylation of calix[4]arene 1c and Gemini 8, 9, 11 with *N*-(3-bromoalkyl)phthalimide. A suspension of **1c** or **8, 9, 11** (4.70 mmol) in dry DMF (80 mL) was stirred for 30 min, then NaH (60 wt.% in oil, 2.3 eq. per OH group) was carefully added. The mixture was stirred for 1 h at room temperature and then *N*-(3-bromoalkyl)phthalimide (2.3 eq. per OH group) was added. After 6 days the reaction was quenched by adding 1 N HCl (70 mL) and the resulting solid was filtered on a Buchner funnel. The collected solid was dissolved in CH₂Cl₂ (70 mL) and was washed with 1 N HCl (3×50 mL). The organic phase was separated, dried over anhydrous Na₂SO₄ and the solvent removed under reduced pressure.

5,11,17,23-Tetra-*n*-hexyl-25,26,27,28-tetrakis(3-phthalimidopropoxy)calix[4]arene (1c).

The crude was purified by flash column chromatography (eluent: hexane/ethyl acetate= 6:4) to obtain the pure product as a white solid in 22% yield.

Mp: 93-94 °C. ¹H NMR (300 MHz, CDCl₃) δ 7.73-7.69 (m, 8H, Pht), 7.61-7.55 (m, 8H, Pht), 6.39 (s, 8H, ArH), 4.37 (d, *J* = 13.2 Hz, 4H, ArCH₂Ar), 3.99 (t, *J* = 7.1 Hz, 8H, OCH₂), 3.88 (t, *J* = 7.1 Hz, 8H, OCH₂CH₂CH₂), 3.06 (d, *J* = 13.2 Hz, 4H, ArCH₂Ar), 2.32 (quint, *J* = 7.1 Hz, 8H, OCH₂CH₂), 2.22 (t, *J* = 7.1 Hz, 8H, ArCH₂), 1.45-1.20 (m, 32H, ArCH₂CH₂CH₂CH₂CH₂), 0.87 (t, *J* = 6.5 Hz, 12H, CH₃). ¹³C NMR (75 MHz, CDCl₃) δ 168.1, 154.0, 136.0, 134.2, 133.4, 132.2, 127.9, 122.9, 72.5, 35.6, 35.1, 31.7, 31.4, 31.0, 29.6, 29.0, 22.6, 14.0. MS (ESI): calculated for [M + Na]⁺ *m/z* = 1531.8, found *m/z* = 1532.1. Elem. Anal. for C₉₆H₁₀₈N₄O₁₂: calc. C 76.36, H 7.21, N 3.71, found C 76.52, H 7.13, N 3.59.

Bis{[2-(3-phthalimidopropoxy)-5-*tert*-butyl-3-methyl]phenyl}methane (17a).

The crude was purified by flash column chromatography (eluent: CH₂Cl₂). The pure compound **17a** was obtained as a white foam in 45% yield.

Mp: 62-63 °C. ¹H NMR (300 MHz, CDCl₃) δ 7.83-7.78 (m, 4H, Pht), 7.71-7.65 (m, 4H, Pht), 6.98 (d, *J* = 2.4 Hz, 2H, ArH), 6.83 (d, *J* = 2.4 Hz, 2H, ArH), 4.01 (s, 2H, ArCH₂Ar), 3.87 (t, *J* = 6.5 Hz, 4H, OCH₂), 3.78 (t, *J* = 6.3 Hz, 4H, OCH₂CH₂CH₂), 2.27 (s, 6H, ArCH₃), 2.14

(quint, $J = 7.7$ Hz, 4H, OCH_2CH_2), 1.18 (s, 18H, *t*Bu). ^{13}C NMR (75 MHz, CDCl_3) δ 168.2, 153.4, 146.0, 133.7, 132.8, 132.1, 129.7, 125.8, 125.5, 123.1, 70.1, 35.6, 34.0, 31.3, 29.5, 29.4, 16.7. MS (ESI): calculated for $[\text{M} + \text{Na}]^+$ $m/z = 737.4$, found $m/z = 737.5$.

Bis{[3-methyl-2-(3-phthalimidopropoxy)]phenyl}methane (17b).

The crude was purified by flash column chromatography (eluent: CH_2Cl_2). The pure compound **17b** was obtained as a white foam in 54% yield.

Mp: 51-52 °C. ^1H NMR (300 MHz, CDCl_3) δ 7.83-7.78 (m, 4H, Pht), 7.71-7.66 (m, 4H, Pht), 6.96-6.78 (m, 6H, *ArH*), 4.01 (s, 2H, ArCH_2Ar), 3.88 (t, $J = 7.1$ Hz, 4H, OCH_2), 3.79 (t, $J = 6.5$ Hz, 4H, $\text{OCH}_2\text{CH}_2\text{CH}_2$), 2.27 (s, 6H, ArCH_3), 2.14 (quint, $J = 7.4$ Hz, 4H, OCH_2CH_2). ^{13}C NMR (75 MHz, CDCl_3) δ 168.2, 155.6, 133.8, 133.7, 132.1, 130.9, 129.2, 128.4, 123.7, 123.1, 70.2, 35.5, 29.6, 29.4, 16.5. MS (ESI): calculated for $[\text{M} + \text{Na}]^+$ $m/z = 625.2$, found $m/z = 625.3$. Elem. Anal. for $\text{C}_{37}\text{H}_{34}\text{N}_2\text{O}_6$: calc. C 73.74, H 5.69, N 4.65, found C 73.70, H 5.71, N 4.72.

Bis{[2-(3-phthalimidopropoxy)-5-hexyl-3-methyl]phenyl}methane (17c). The crude was purified by flash column chromatography (eluent: CH_2Cl_2). The pure compound **17c** was obtained as a colourless oil in 38% yield.

^1H NMR (300 MHz, CDCl_3) δ 7.84-7.75 (m, 4H, Pht), 7.71-7.63 (m, 4H, Pht), 6.76 (d, $J = 1.9$ Hz, 2H, *ArH*), 6.60 (d, $J = 1.9$ Hz, 2H, *ArH*), 3.96 (s, 2H, ArCH_2Ar), 3.88 (t, $J = 7.1$ Hz, 4H, OCH_2), 3.76 (t, $J = 6.3$ Hz, 4H, $\text{OCH}_2\text{CH}_2\text{CH}_2$), 2.39 (t, $J = 7.5$ Hz, 4H, ArCH_2), 2.25 (s, 6H, ArCH_3), 2.12 (quint, $J = 7.4$ Hz, 4H, OCH_2CH_2), 1.53-1.42 (m, 4H, ArCH_2CH_2), 1.36-1.18 (m, 12H, $\text{ArCH}_2\text{CH}_2\text{CH}_2\text{CH}_2\text{CH}_2$), 0.85 (t, $J = 6.4$ Hz, 6H, CH_2CH_3). ^{13}C NMR (75 MHz, CDCl_3) δ 168.2, 153.5, 138.0, 133.7, 133.4, 132.1, 130.3, 128.9, 128.3, 123.1, 70.1, 35.5, 35.2, 31.6, 31.5, 29.4, 28.9, 22.5, 16.5, 14.0. MS (ESI): calculated for $[\text{M} + \text{Na}]^+$ $m/z = 793.4$, found $m/z = 793.6$.

Synthesis of Bis[(2-hexyloxy-3-methyl-5-*tert*-butyl)phenyl]methane (21).

The product was obtained according to the literature procedure of alkylation of calixarenes.¹⁹ A suspension of Gemini **8** (0.8 g, 2.35 mmol) in dry DMF (24 mL) was stirred for 30 min and then, at 0 °C, NaH (60 wt.-% in oil, 0.57 g, 14.12 mmol) was added. The mixture was stirred for 0.5 h and then 1-iodohexane 98+% (2.13 mL, 14.12 mmol) was added. After 1 h the ice bath was removed and the reaction mixture was stirred for one day.

The reaction was quenched with 1 N HCl (70 mL) and the resulting solid filtered on a Büchner funnel. The crude product was dissolved in CH₂Cl₂ (70 mL) and washed with 1 N HCl (3×50 mL). The organic phase was separated, dried over anhydrous Na₂SO₄ and evaporated under reduced pressure to obtain a yellowish oil. The residue was purified by flash column chromatography on silica gel (eluent: CH₂Cl₂ and CH₂Cl₂/MeOH= 99:1) to obtain the pure product as a colourless oil in 90% yield.

¹H NMR (300 MHz, CDCl₃) δ 7.12 (d, *J* = 2.3 Hz, 2H, Ar*H*), 6.98 (d, *J* = 2.3 Hz, 2H, Ar*H*), 4.16 (s, 2H, ArCH₂Ar), 3.82 (t, *J* = 6.7 Hz, 4H, OCH₂), 2.40 (s, 6H, ArCH₃), 1.86 (quint, *J* = 7.0 Hz, 4H, OCH₂CH₂), 1.55 (bquint, 4H, OCH₂CH₂), 1.49-1.32 (m, 12H, OCH₂CH₂CH₂CH₂CH₂), 1.31 (s, 18H, *t*Bu), 0.99 (t, *J* = 6.8 Hz, 6H, CH₂CH₃). ¹³C NMR (75 MHz, CDCl₃) δ 153.8, 145.8, 133.1, 129.8, 125.7, 125.6, 72.8, 34.1, 31.8, 31.5, 30.5, 29.6, 25.9, 22.7, 16.7, 14.1. MS (ESI): calculated for [M + Na]⁺ *m/z* = 531.4, found *m/z* = 531.5.

Synthesis of Bis(2-hexyloxy-3-methyl-5-nitrophenyl)methane (22).

The product was obtained according to the general procedure for the ipso nitration of calixarenes.²⁰ To a solution of **21** (1.05 g, 2.065 mmol) in trifluoroacetic acid (4.7 mL, 61.17 mmol), NaNO₃ (3.45 g, 40.7 mmol) was added and the mixture turned orange. After one night the reaction was stopped with addition of water (100 mL) and extracted with CH₂Cl₂ (2×50 mL). The separated organic layer was washed with water (75 mL), dried over anhydrous Na₂SO₄ and concentrated under reduced pressure. The residue was purified by flash column chromatography on silica gel (eluent: hexane/ethyl acetate= 98:2) to obtain the pure product as a light yellow oil in 60% yield.

¹H NMR (300 MHz, CDCl₃) δ 7.99 (d, *J* = 2.8 Hz, 2H, Ar*H*), 7.77 (d, *J* = 2.8 Hz, 2H, Ar*H*), 4.10 (s, 2H, ArCH₂Ar), 3.81 (t, *J* = 6.6 Hz, 4H, OCH₂), 2.38 (s, 6H, ArCH₃), 1.79 (quint, *J* = 6.6 Hz, 4H, OCH₂CH₂), 1.47-1.37 (m, 4H, OCH₂CH₂CH₂), 1.37-1.29 (m, 8H, OCH₂CH₂CH₂CH₂CH₂), 0.89 (t, *J* = 6.7 Hz, 6H, CH₃). ¹³C NMR (75 MHz, CDCl₃) δ 161.4, 143.5, 134.0, 132.8, 125.3, 123.6, 73.4, 31.6, 30.3, 30.2, 25.6, 22.5, 16.8, 13.9. MS (ESI): calculated for [M + Na]⁺ *m/z* = 509.3, found *m/z* = 509.4.

Synthesis of 5,11,17,23-Tetra-*t*-butyl-25,26,27,28-tetrakis(3-aminopropoxy)calix[4]arene (3a) and 25,26,27,28-tetrakis(3-aminopropoxy)calix[4]arene (3b) were synthesized according to literature procedures.^{6b,6c}

General procedure for the removal of the phthaloyl protecting groups.

A solution of calix[4]arene **2c** or linear compound **17a-c** (1.70 mmol) and hydrazine monohydrate (50 eq. per phthalimide group) in ethanol (50 mL) was refluxed overnight. The solvent was then removed under reduced pressure. The residue was dissolved in CH₂Cl₂ (50 mL) and washed with water (40 mL). The organic layer was separated and the water phase was extracted with CH₂Cl₂ (3×40 mL). The combined organic layers were dried over anhydrous Na₂SO₄ and the pure compounds were obtained after evaporation of the solvent under reduced pressure.

5,11,17,23-Tetra-*n*-hexyl-25,26,27,28-tetrakis(3-aminopropoxy)calix[4]arene (3c). The pure compound was obtained as a light yellow oil in 65% yield.

¹H NMR (300 MHz, CDCl₃) δ 6.42 (s, 8H, ArH), 4.29 (d, *J* = 12.8 Hz, 4H, ArCH₂Ar), 3.88 (t, *J* = 6.9 Hz, 8H, OCH₂), 3.04 (d, *J* = 12.8 Hz, 4H, ArCH₂Ar), 2.88 (t, *J* = 6.9 Hz, 8H, OCH₂CH₂CH₂), 3.05 (bs, 8H, NH₂), 2.24 (t, *J* = 7.3 Hz, 8H, ArCH₂), 2.06 (quint, *J* = 6.9 Hz, 8H, OCH₂CH₂), 1.50-1.15 (m, 32H, ArCH₂CH₂CH₂CH₂CH₂), 0.88 (t, *J* = 6.8 Hz, 12H, CH₃). ¹³C NMR (75 MHz, CDCl₃) δ 153.9, 136.0, 134.2, 127.9, 72.6, 39.2, 35.1, 33.7, 31.7, 31.4, 30.8, 29.6, 29.0, 22.7, 14.1. MS (ESI): calculated for [M + H]⁺ *m/z* = 989.9, found *m/z* = 990.0, calculated for [M + Na]⁺ *m/z* = 1011.8, found *m/z* = 1011.9. Elem. Anal. for C₆₄H₁₀₀N₄O₄: calc. C 77.68, H 10.19, N 5.66, found C 77.52, H 10.21, N 5.79.

Bis[2-(3-aminopropoxy)-5-*tert*-butyl-3-methylphenyl]methane (18a).

The pure compound was obtained as a colourless oil in quantitative yield.

¹H NMR (300 MHz, CDCl₃) δ 7.02 (d, 2H, *J* = 2.4 Hz, ArH), 6.86 (d, 2H, *J* = 2.4 Hz, ArH), 4.04 (s, 2H, ArCH₂Ar), 3.77 (t, *J* = 6.2 Hz, 4H, OCH₂), 2.90 (t, *J* = 6.8 Hz, 4H, OCH₂CH₂CH₂), 2.30 (s, 6H, ArCH₃), 1.88 (quint, *J* = 6.5 Hz, 4H, OCH₂CH₂), 1.40 (bs, 4H, NH₂). ¹³C NMR (75 MHz, CDCl₃) δ 153.5, 146.0, 132.8, 129.8, 125.8, 125.5, 70.6, 39.5, 34.2, 34.1, 31.3, 29.6, 16.6. MS (ESI): calculated for [M + H]⁺ *m/z* = 477.3, found *m/z* = 477.4.

Bis[2-(3-aminopropoxy)-3-methylphenyl]methane (18b).

The pure compound was obtained as a colourless oil in 62% yield.

¹H NMR (300 MHz, CDCl₃) δ 7.04-6.84 (m, 6H, ArH), 4.05 (s, 2H, ArCH₂Ar), 3.80 (t, *J* = 6.2 Hz, 4H, OCH₂), 2.91 (t, *J* = 6.8 Hz, 4H, OCH₂CH₂CH₂), 2.30 (s, 6H, ArCH₃), 1.89 (quint,

$J = 6.5$ Hz, 4H, OCH₂CH₂), 1.60 (bs, 4H, NH₂). ¹³C NMR (75 MHz, CDCl₃) δ 155.7, 133.8, 130.9, 129.2, 128.4, 123.8, 70.7, 39.4, 34.1, 29.4, 16.3. MS (ESI): calculated for [M + H]⁺ m/z = 343.2, found m/z = 343.3. Elem. Anal. for C₂₁H₃₀N₂O₂: calc. C 73.65, H 8.83, N 8.18, found C 73.73, H 8.94, N 8.25.

Bis[2-(3-aminopropoxy)-5-hexyl-3-methylphenyl]methane (18c).

The pure compound was obtained as a colourless oil in quantitative yield.

¹H NMR (300 MHz, CDCl₃) δ 6.84 (s, 2H, ArH), 6.64 (s, 2H, ArH), 3.99 (s, 2H, ArCH₂Ar), 3.75 (t, $J = 6.1$ Hz, 4H, OCH₂), 2.90 (bs, 4H, OCH₂CH₂CH₂), 2.43 (t, $J = 7.3$ Hz, 4H, ArCH₂), 2.27 (s, 6H, ArCH₃), 2.00 (bs, 4H, NH₂), 1.95-1.80 (m, 4H, OCH₂CH₂), 1.60-1.42 (m, 4H, ArCH₂CH₂), 1.42-1.22 (m, 12H, ArCH₂CH₂CH₂CH₂CH₂), 0.85 (t, $J = 6.7$ Hz, CH₂CH₃). ¹³C NMR (75 MHz, CDCl₃) δ 153.6, 138.1, 133.3, 130.3, 129.0, 128.3, 70.7, 39.5, 35.2, 34.1, 31.6, 31.5, 29.3, 28.9, 22.5, 16.4, 14.0. MS (ESI): calculated for [M + H]⁺ m/z = 511.4, found m/z = 511.5.

Bis(5-amino-2-hexyloxy-3-methylphenyl)methane (23).

The product was obtained according to the general procedure for the nitro reduction of calixarenes.¹⁹ To a solution of **22** (0.22 g, 0.45 mmol) and hydrazine monohydrate (0.22 mL, 4.52 mmol) in ethanol (14 mL), a catalytic amount of Pd/C was added and the reaction mixture was stirred and refluxed overnight. The solvent was then removed under reduced pressure, the residue dissolved in CH₂Cl₂ (50 mL) and the catalyst filtered off through a paper filter. The organic layer was dried over anhydrous Na₂SO₄ and pure amine **23** was obtained after evaporation of the solvent under reduced pressure as a light yellow oil in 78% yield.

¹H NMR (300 MHz, CDCl₃) δ 6.35 (d, $J = 2.6$ Hz, 2H, ArH), 6.19 (d, $J = 2.6$ Hz, 2H, ArH), 3.90 (s, 2H, ArCH₂Ar), 3.69 (t, $J = 6.6$ Hz, 4H, OCH₂), 3.32 (bs, 4H, NH₂), 2.23 (s, 6H, ArCH₃), 1.76 (quint, $J = 6.9$ Hz, 4H, OCH₂CH₂), 1.51-1.41 (m, 4H, OCH₂CH₂CH₂), 1.35-1.28 (m, 8H, OCH₂CH₂CH₂CH₂CH₂), 0.91 (t, $J = 6.7$ Hz, 6H, CH₂CH₃). ¹³C NMR (75 MHz, CDCl₃) δ 148.5, 142.0, 134.6, 131.4, 115.7, 115.0, 73.2, 31.8, 30.3, 29.6, 29.0, 25.8, 22.6, 16.4, 14.0. MS (ESI): calculated for [M + H]⁺ m/z = 427.3, found m/z = 427.5, calculated for [M + Na]⁺ m/z = 449.3, found m/z = 449.5.

General procedure for the guanidilation of calix[4]arenes 3a-c and linear compounds 18a-c.

To a solution of calix[4]arenes **3a-c** or non-macrocyclic compounds **18a-c** (0.168 mmol) in dry CH₂Cl₂ (4.5 mL), N,N'-Bis(*tert*-butoxycarbonyl)-N''-triflylguanidine (97%) (0.91 eq. per NH₂ group) was added and the mixture was stirred for 5 h. Another 0.5 eq. aliquot of N,N'-Bis(*tert*-butoxycarbonyl)-N''-triflylguanidine was then added and after 5 h the mixture was transferred to a separatory funnel and washed with 2 M aqueous sodium bisulfate (5 mL) and with saturated sodium bicarbonate (5 mL). Each aqueous layer was extracted with CH₂Cl₂ (2×5 mL). The combined organic phases were washed with brine (5 mL), dried over anhydrous Na₂SO₄ and concentrated under reduced pressure.

5,11,17,23-Tetra-*tert*-butyl-25,26,27,28-tetrakis[3-(bis-Boc-guanidine)propoxy]calix[4]arene (4a). The residue was purified by flash column chromatography on silica gel (eluent: from CH₂Cl₂ to CH₂Cl₂/MeOH= 99:1) to obtain the pure product as a colourless oil in 63% yield.

¹H NMR (300 MHz, CDCl₃) δ 11.49 (s, 4H, BocNH), 8.37 (t, *J* = 4.8 Hz, 4H, CH₂NH), 6.77 (s, 8H, ArH), 4.33 (d, *J* = 12.6 Hz, 4H, ArCH₂Ar), 3.95 (t, *J* = 7.2 Hz, 8H, OCH₂), 3.58 (quint, *J* = 5.9 Hz, 8H, OCH₂CH₂CH₂), 3.14 (d, *J* = 12.6 Hz, 4H, ArCH₂Ar), 2.27 (quint, *J* = 7.2 Hz, 8H, OCH₂CH₂), 1.47 (s, 36H, *t*Bu), 1.46 (s, 36H, *t*Bu), 1.07 (s, 36H, *t*Bu). ¹³C NMR (75 MHz, CDCl₃) δ 163.6, 156.1, 153.2, 153.0, 144.5, 133.6, 125.0, 82.8, 78.9, 72.3, 38.0, 33.7, 31.3, 31.0, 29.8, 28.2, 28.0. MS (ESI): calculated for [M + H]⁺ *m/z* = 1846.2, found *m/z* = 1846.4, calculated for [M + Na]⁺ *m/z* = 1868.1, found *m/z* = 1868.3. Elem. Anal. for C₁₀₀H₁₅₆N₁₂O₂₀: calc. C 65.05, H 8.52, N 9.10, found C 64.98, H 8.71, N 8.99.

25,26,27,28-Tetrakis[3-(bis-Boc-guanidine)propoxy]calix[4]arene (4b). The residue was purified by flash column chromatography on silica gel (eluent: from CH₂Cl₂ to CH₂Cl₂/MeOH= 99:1) to obtain the pure product as a colourless oil in 62% yield.

¹H NMR (300 MHz, CDCl₃) δ 11.48 (s, 4H, BocNH), 8.38 (t, *J* = 5.2 Hz, 4H, CH₂NH), 6.61-6.53 (m, 12H, ArH), 4.38 (d, *J* = 13.4 Hz, 4H, ArCH₂Ar), 3.97 (t, *J* = 7.1 Hz, 8H, OCH₂), 3.56 (quint, *J* = 5.9 Hz, 8H, OCH₂CH₂CH₂), 3.18 (d, *J* = 13.4 Hz, 4H, ArCH₂Ar), 2.18 (quint, *J* = 7.1 Hz, 8H, OCH₂CH₂), 1.47 (s, 36H, *t*Bu), 1.46 (s, 36H, *t*Bu). ¹³C NMR (75 MHz, CDCl₃) δ 163.6, 156.1, 156.0, 153.2, 134.9, 128.3, 122.3, 82.9, 79.0, 72.1, 37.9, 31.0, 29.9, 28.3, 28.1. MS (ESI): calculated for [M + H]⁺ *m/z* = 1621.9, found *m/z* = 1621.8, calculated for [M + Na]⁺ *m/z* = 1643.9, found *m/z* = 1643.9. Elem. Anal. for C₈₄H₁₂₄N₁₂O₂₀: calc. C 62.20, H 7.71, N 10.36, found C 62.34, H 7.87, N 10.16.

5,11,17,23-Tetra-*n*-hexyl-25,26,27,28-tetrakis[3-(bis-Boc-

guanidine)propoxy]calix[4]arene (4c). The residue was purified by flash column chromatography on silica gel (eluent: from CH₂Cl₂ to CH₂Cl₂/MeOH= 99:1) to obtain the pure product as a colourless oil in 95% yield.

¹H NMR (300 MHz, CDCl₃) δ 11.48 (s, 4H, BocNH), 8.37 (t, *J* = 4.9 Hz, 4H, CH₂NH), 6.41 (s, 12H, ArH), 4.28 (d, *J* = 13.2 Hz, 4H, ArCH₂Ar), 3.91 (t, *J* = 6.8 Hz, 8H, OCH₂), 3.55-3.53 (m, 8H, OCH₂CH₂CH₂), 3.07 (d, *J* = 13.2 Hz, 4H, ArCH₂Ar), 2.23-2.16 (m, 16H, OCH₂CH₂ and ArCH₂), 1.65-1.20 (m, 32H, ArCH₂CH₂CH₂CH₂CH₂), 1.45 (s, 36H, *t*Bu), 1.46 (s, 36H, *t*Bu), 0.87 (t, *J* = 6.4 Hz, 12H, CH₃). ¹³C NMR (75 MHz, CDCl₃) δ 163.5, 156.1, 153.7, 153.1, 136.1, 134.1, 128.0, 82.8, 78.8, 72.1, 37.9, 35.1, 31.7, 31.4, 30.9, 29.8, 29.0, 28.2, 28.0, 22.6, 14.1. MS (ESI): calculated for [M + Na]⁺ *m/z* = 1980.3, found *m/z* = 1980.3. Elem. Anal. for C₁₀₈H₁₇₂N₁₂O₂₀: calc. C 66.23, H 8.85, N 8.58, found C 66.15, H 8.99, N 8.47.

Bis{3-methyl-2-[3-(bis-Boc-guanidine)propoxy]-5-*tert*-butylphenyl}methane (19a).

The crude was purified by flash column chromatography on silica gel (eluent: from CH₂Cl₂ to CH₂Cl₂/MeOH= 99:1) to obtain the pure product as a colourless oil in 94% yield.

¹H NMR (300 MHz, CDCl₃) δ 11.49 (bs, 2H, BocNH), 8.51 (t, *J* = 5.2 Hz, 2H, CH₂NH), 7.01 (d, 2H, *J* = 2.3 Hz, ArH), 6.85 (d, 2H, *J* = 2.3 Hz, ArH), 4.00 (s, 2H, ArCH₂Ar), 3.76 (t, *J* = 6.1 Hz, 4H, OCH₂), 3.62 (q, *J* = 6.8 Hz, 4H, OCH₂CH₂CH₂), 2.28 (s, 6H, ArCH₃), 2.00 (quint, *J* = 6.6 Hz, 4H, OCH₂CH₂), 1.49 (s, 18H, *t*BuBoc), 1.47 (s, 18H, *t*BuBoc), 1.19 (s, 18H, *t*Bu). ¹³C NMR (75 MHz, CDCl₃) δ 163.6, 156.1, 153.3, 153.1, 146.0, 132.8, 129.8, 125.9, 125.5, 82.8, 79.0, 69.8, 38.1, 34.0, 31.3, 29.8, 29.7, 28.2, 28.0, 16.7. MS (ESI): calculated for [M + Na]⁺ *m/z* = 961.6, found *m/z* = 961.6.

Bis{3-methyl-2-[3-(bis-Boc-guanidine)propoxy]phenyl}methane (19b).

The crude was purified by flash column chromatography on silica gel (eluent: from CH₂Cl₂ to CH₂Cl₂/MeOH= 99:1) to obtain the pure product as a colourless oil in 98% yield.

¹H NMR (300 MHz, CDCl₃) δ 11.48 (bs, 2H, BocNH), 8.55 (t, *J* = 5.0 Hz, 2H, CH₂NH), 7.03-6.83 (m, 6H, ArH), 4.01 (s, 2H, ArCH₂Ar), 3.79 (t, *J* = 6.2 Hz, 4H, OCH₂), 3.63 (quint, *J* = 5.4 Hz, 4H, OCH₂CH₂CH₂), 2.29 (s, 6H, ArCH₃), 2.02 (quint, *J* = 6.5 Hz, 4H, OCH₂CH₂), 1.49 (s, 18H, *t*Bu), 1.46 (s, 18H, *t*Bu). ¹³C NMR (75 MHz, CDCl₃) δ 163.6, 156.1, 155.5, 153.1, 133.8, 130.9, 129.2, 128.4, 123.8, 82.9, 79.1, 70.0, 38.1, 29.7, 29.5, 28.2,

28.0, 16.4. MS (ESI): calculated for $[M + Na]^+$ $m/z = 849.5$, found $m/z = 849.5$. Elem. Anal. for $C_{43}H_{66}N_6O_{10}$: calc. C 62.45, H 8.04, N 10.16, found C 62.51, H 8.06, N 10.19.

Bis{3-methyl-2-[3-(bis-Boc-guanidine)propoxy]-5-hexylphenyl}methane (19c).

The crude was purified by flash column chromatography on silica gel (eluent: CH_2Cl_2 and $CH_2Cl_2/MeOH = 99:1$) to obtain the pure product as a colourless oil in 88% yield.

1H NMR (300 MHz, $CDCl_3$) δ 11.49 (bs, 2H, BocNH), 8.53 (t, $J = 5.1$ Hz, 2H, CH_2NH), 6.82 (d, $J = 1.8$ Hz, 2H, ArH), 6.63 (d, $J = 1.8$ Hz, 2H, ArH), 3.96 (s, 2H, Ar CH_2 Ar), 3.74 (t, $J = 6.1$ Hz, 4H, O CH_2), 3.61 (q, $J = 5.6$ Hz, 4H, O $CH_2CH_2CH_2$), 2.42 (t, $J = 7.5$ Hz, 4H, Ar CH_2), 2.26 (s, 6H, Ar CH_3), 1.99 (quint, $J = 6.6$ Hz, 4H, O CH_2CH_2), 1.49-1.46 (m, 4H, Ar CH_2CH_2), 1.49 (s, 18H, *t*Bu), 1.46 (s, 18H, *t*Bu), 1.29-1.25 (m, 12H, Ar $CH_2CH_2CH_2CH_2CH_2$), 0.85 (t, $J = 6.5$ Hz, 6H, CH_2CH_3). ^{13}C NMR (75 MHz, $CDCl_3$) δ 163.6, 156.1, 153.5, 153.1, 138.0, 133.4, 130.3, 129.0, 128.3, 82.9, 79.1, 69.9, 38.1, 35.2, 31.6, 31.5, 29.7, 29.4, 28.9, 28.2, 28.0, 22.5, 16.4, 14.0. MS (ESI): calculated for $[M + H]^+$ $m/z = 995.7$, found $m/z = 995.9$.

Synthesis of Bis{2-hexyloxy-3-methyl-5-(bis-Boc-guanidine)phenyl}methane (24).

To a solution of Gemini **23** (50 mg, 0.12 mmol) in dry CH_2Cl_2 (3 mL), Et_3N (35 μ L, 0.25 mmol) and *N,N'*-Bis(*tert*-butoxycarbonyl)-*N''*-triflylguanidine (91 mg, 0.24 mmol) were added and the mixture was stirred overnight. Another aliquot of Et_3N (17 μ L, 0.12 mmol) and of *N,N'*-Bis(*tert*-butoxycarbonyl)-*N''*-triflylguanidine (40 mg, 0.065 mmol) were subsequently added. After other 7 h the mixture was transferred to a separatory funnel and the organic layer washed with 2 M aqueous sodium bisulfate (5 mL) and with a saturated sodium bicarbonate aqueous solution (5 mL). Each aqueous layer was extracted with $CHCl_3$ (2 \times 5 mL). The combined organic phases were washed with brine (5 mL), dried over anhydrous Na_2SO_4 and concentrated under reduced pressure. The residue was purified by flash column chromatography on silica gel (eluent: hexane/ $CH_2Cl_2 = 1:1$) to obtain the pure product as a colorless oil in 42% yield.

1H NMR (300 MHz, $CDCl_3$) δ 11.61 (bs, 2H, BocNH), 10.03 (s, 2H, ArNH), 7.37 (d, $J = 2.4$ Hz, 2H, ArH), 6.81 (d, $J = 2.4$ Hz, 2H, ArH), 3.98 (s, 2H, Ar CH_2 Ar), 3.67 (t, $J = 6.5$ Hz, 4H, O CH_2), 2.28 (s, 6H, Ar CH_3), 1.73 (quint, $J = 6.8$ Hz, 4H, O CH_2CH_2), 1.58-1.25 (m, 4H, O $CH_2CH_2CH_2CH_2CH_2$), 1.50 (s, 18H, *t*Bu), 1.46 (s, 18H, *t*Bu), 0.89 (t, $J = 6.5$ Hz, 6H, CH_2CH_3). ^{13}C NMR (75 MHz, $CDCl_3$) δ 153.5, 153.2, 152.8, 134.1, 131.9, 131.4, 123.7,

122.4, 83.4, 79.2, 72.9, 31.7, 30.3, 29.4, 28.1, 28.0, 25.8, 22.6, 16.6, 14.0. MS (ESI): calculated for $[M + Na]^+$ $m/z = 933.6$, found $m/z = 933.6$.

General procedure for the removal of the Boc protecting groups.

Concentrated HCl (1 equiv for each Boc group) was added dropwise to a solution of the protected guanidinium calix[4]arenes **4a-c** or Gemini derivatives **19a-c** and **24** in 1,4-dioxane (0.1 mmol/10 mL). The reaction mixture was stirred for 24-72 h, and the solvent was removed under reduced pressure to obtain the pure product.

5,11,17,23-Tetra-*tert*-butyl-25,26,27,28-tetrakis(3-guanidiniumpropoxy)calix[4]arene, tetrachloride (**5a**).

The pure compound was obtained as a white powder in quantitative yield. Hygroscopic.

Mp: > 250 °C dec. ^1H NMR (300 MHz, CD_3OD) δ 6.84 (m, 8H, *ArH*), 4.39 (d, $J = 12.5$ Hz, 4H, ArCH_2Ar), 4.02 (t, $J = 7.5$ Hz, 8H, OCH_2), 4.02 (t, $J = 7.5$ Hz, 8H, $\text{OCH}_2\text{CH}_2\text{CH}_2$), 3.19 (d, $J = 12.5$ Hz, 4H, ArCH_2Ar), 2.32 (quint, $J = 7.5$ Hz, 8H, OCH_2CH_2), 1.08 (s, 36H, *t*Bu). ^1H NMR (300 MHz, D_2O) δ 7.02 (m, 8H, *ArH*), 4.33 (d, $J = 12.3$ Hz, 4H, ArCH_2Ar), 3.99 (t, $J = 7.7$ Hz, 8H, OCH_2), 3.38-3.29 (m, 12H, $\text{OCH}_2\text{CH}_2\text{CH}_2$ and ArCH_2Ar), 2.29-2.25 (m, 8H, OCH_2CH_2), 1.10 (s, 36H, *t*Bu). ^{13}C NMR (75 MHz, CD_3OD) δ 158.7, 154.4, 146.1, 135.0, 126.4, 73.4, 40.0, 34.8, 32.3, 32.0, 30.9. MS (ESI): calculated for $[M + H - 4\text{HCl}]^+$ $m/z = 1045.7$, found $m/z = 1045.7$. Elem. Anal. for $\text{C}_{60}\text{H}_{96}\text{N}_{12}\text{O}_4\text{Cl}_4 \times 4\text{H}_2\text{O}$: calc. C 57.04, H 8.30, N 13.30; found C 56.90, H 7.95, N 12.92.

25,26,27,28-Tetrakis(3-guanidiniumpropoxy)calix[4]arene, tetrachloride (5b**)**. The pure compound was obtained as a white powder in quantitative yield. Hygroscopic.

Mp: > 250 °C dec. ^1H NMR (300 MHz, CD_3OD) δ 6.68-6.54 (m, 12H, *ArH*), 4.41 (d, $J = 13.3$ Hz, 4H, ArCH_2Ar), 4.08 (t, $J = 7.0$ Hz, 8H, OCH_2), 3.39 (bt, 8H, $\text{OCH}_2\text{CH}_2\text{CH}_2$), 4.41 (d, $J = 13.3$ Hz, 4H, ArCH_2Ar), 2.24 (quint, $J = 6.9$ Hz, 8H, OCH_2CH_2). ^1H NMR (300 MHz, D_2O) δ 6.86-6.70 (m, 12H, *ArH*), 4.40 (d, $J = 13.3$ Hz, 4H, ArCH_2Ar), 4.08 (t, $J = 7.0$ Hz, 8H, OCH_2), 3.40-3.33 (m, 12H, $\text{OCH}_2\text{CH}_2\text{CH}_2$, ArCH_2Ar), 2.25 (quint, $J = 6.9$ Hz, 8H, OCH_2CH_2). ^{13}C NMR (75 MHz, CD_3OD) δ 158.7, 157.2, 136.0, 129.6, 123.6, 73.2, 40.0, 32.1, 30.9. MS (ESI): calculated for $[M + H - 4\text{HCl}]^+$ $m/z = 843.6$, found $m/z = 843.6$. Elem. Anal. for $\text{C}_{44}\text{H}_{64}\text{N}_{12}\text{O}_4\text{Cl}_4 \times 4\text{H}_2\text{O}$: calc. C 54.66, H 6.67, N 17.38, found C 54.51, H 6.49, N 17.28.

5,11,17,23-Tetra-*n*-hexyl-25,26,27,28-tetrakis(3-guanidiniumpropoxy)calix[4]arene, tetrachloride (5c). The pure compound was obtained as a white powder in quantitative yield. Hygroscopic.

Mp: >250 °C dec. ¹H NMR (300 MHz, CD₃OD) δ 7.75 (t, *J* = 5.4 Hz, 4H, NHCH₂), 6.47 (s, 8H, ArH), 4.35 (d, *J* = 13.0 Hz, 4H, ArCH₂Ar), 3.99 (t, *J* = 7.2 Hz, 8H, OCH₂), 3.46-3.35 (m, 8H, OCH₂CH₂CH₂), 3.13 (d, *J* = 13.0 Hz, 4H, ArCH₂Ar), 2.32-2.15 (m, 16H, OCH₂CH₂ and ArCH₂), 1.50-1.16 (m, 32H, ArCH₂CH₂CH₂CH₂CH₂), 0.89 (t, *J* = 6.5 Hz, 12H, CH₃). ¹H NMR (300 MHz, D₂O, 353 K) δ 6.49 (bs, 8H, ArH), 4.42 (bs, 4H, ArCH₂Ar), 4.08 (bs, 8H, OCH₂), 3.45 (bs, 8H, OCH₂CH₂CH₂), 3.21 (bs, 4H, ArCH₂Ar), 2.31 (bs, 16H, OCH₂CH₂ and ArCH₂), 1.60-1.20 (bs, 32H, ArCH₂CH₂CH₂CH₂CH₂), 0.96 (bs, 12H, CH₃). ¹³C NMR (75 MHz, CD₃OD) δ 159.0, 155.4, 137.8, 135.8, 129.7, 73.5, 40.3, 36.6, 33.3, 33.1, 32.3, 31.1, 30.3, 24.2, 14.9. MS (ESI): calculated for [M + H - 4HCl]⁺ *m/z* = 1157.8, found *m/z* = 1158.0. Elem. Anal. for C₆₈H₁₁₂N₁₂O₄Cl₄×4H₂O: calc. C 59.37, H 8.79, N 12.22, found C 59.14, H 8.52, N 12.03.

Bis[5-*tert*-butyl-2-(3-guanidiniumpropoxy)-3-methylphenyl]methane, dichloride (20a).

The pure compound was obtained as a white powder in quantitative yield. Hygroscopic.

Mp: > 250 °C dec. ¹H NMR (300 MHz, CD₃OD) δ 7.08 (d, *J* = 2.3 Hz, 2H, ArH), 6.93 (s, 2H, ArH), 4.02 (s, 2H, ArCH₂Ar), 3.80 (t, *J* = 5.9 Hz, 4H, OCH₂), 3.41 (t, *J* = 6.8 Hz, 4H, OCH₂CH₂CH₂), 2.29 (s, 6H, ArCH₃), 2.04 (quint, *J* = 6.3 Hz, 4H, OCH₂CH₂), 1.19 (s, 18H, *t*Bu). ¹H NMR (300 MHz, D₂O) δ 7.21 (s, 2H, ArH), 6.93 (s, 2H, ArH), 4.01 (s, 2H, ArCH₂Ar), 3.79 (bt, 4H, OCH₂), 3.35 (t, *J* = 6.0 Hz, 4H, OCH₂CH₂CH₂), 2.27 (s, 6H, ArCH₃), 2.07-1.90 (m, 4H, OCH₂CH₂), 1.17 (s, 18H, *t*Bu). ¹³C NMR (75 MHz, CD₃OD) δ 159.0, 154.7, 148.1, 134.4, 131.5, 127.6, 127.0, 71.0, 40.3, 35.3, 32.1, 31.2, 30.8, 28.4, 17.1. MS (ESI): calculated for [M + H - 2HCl]⁺ *m/z* = 539.4, found *m/z* = 539.5.

Bis{[2-(3-guanidiniumpropoxy)-3-methyl]phenyl}methane, dichloride (20b). The pure compound was obtained as a white powder in quantitative yield. Hygroscopic.

Mp: > 250 °C dec. ¹H NMR (300 MHz, CD₃OD) δ 7.06 (dd, *J* = 7.4 Hz, *J* = 1.1 Hz, 2H, ArH), 6.92 (t, *J* = 7.4 Hz, 2H, ArH), 6.84 (dd, *J* = 7.4 Hz, *J* = 1.1 Hz, 2H, ArH), 4.03 (s, 2H, ArCH₂Ar), 3.82 (t, *J* = 6.1 Hz, 4H, OCH₂), 3.39 (t, *J* = 6.9 Hz, 4H, OCH₂CH₂CH₂), 2.29 (s, 6H, ArCH₃), 2.03 (quint, *J* = 6.4 Hz, 4H, OCH₂CH₂). ¹H NMR (300 MHz, D₂O) δ 7.17 (d, *J*

= 7.4 Hz, 2H, ArH), 7.00 (t, $J = 7.4$ Hz, 2H, ArH), 6.88 (d, $J = 7.4$ Hz, 2H, ArH), 3.99 (s, 2H, ArCH₂Ar), 3.82 (t, $J = 6.2$ Hz, 4H, OCH₂), 3.33 (t, $J = 6.7$ Hz, 4H, OCH₂CH₂CH₂), 2.29 (s, 6H, ArCH₃), 2.02 (quint, $J = 6.4$ Hz, 4H, OCH₂CH₂). ¹³C NMR (75 MHz, CD₃OD) δ 159.0, 156.9, 135.3, 132.4, 130.9, 130.0, 125.6, 71.0, 68.4, 40.2, 31.1, 30.8, 21.1, 16.9. MS (ESI): calculated for [M + H - 2HCl]⁺ $m/z = 427.3$, found $m/z = 427.5$. Elem. Anal. for C₂₃H₃₆N₆O₂Cl₂×2H₂O: calc. C 51.59, H 7.53, N 15.69, found C 51.72, H 7.66, N 15.58.

Bis[2-(3-guanidiniumpropoxy)-5-hexyl-3-methylphenyl]methane, dichloride (20c).

The pure compound was obtained as a white powder in 76% yield.

Mp: > 250 °C dec. ¹H NMR (300 MHz, CD₃OD) δ 7.44 (t, $J = 5.1$ Hz, 2H, CH₂NH), 6.86 (d, $J = 1.9$ Hz, 2H, ArH), 6.63 (d, $J = 1.9$ Hz, 2H, ArH), 3.98 (s, 2H, ArCH₂Ar), 3.78 (t, $J = 5.9$ Hz, 4H, OCH₂), 3.42-3.32 (m, 4H, OCH₂CH₂CH₂), 2.43 (t, $J = 7.3$ Hz, 4H, ArCH₂), 2.27 (s, 6H, ArCH₃), 2.02 (quint, $J = 6.3$ Hz, 4H, OCH₂CH₂), 1.55-1.40 (m, 4H, ArCH₂CH₂), 1.32-1.16 (m, 12H, ArCH₂CH₂CH₂CH₂CH₂), 0.86 (t, $J = 6.5$ Hz, 6H, CH₂CH₃). ¹H NMR (300 MHz, D₂O) δ 7.07 (s, 2H, ArH), 6.78 (s, 2H, ArH), 3.99 (s, 2H, ArCH₂Ar), 3.82 (t, $J = 6.6$ Hz, 4H, OCH₂), 3.35 (t, $J = 6.9$ Hz, 4H, OCH₂CH₂CH₂), 2.52 (t, $J = 6.9$ Hz, 4H, ArCH₂), 2.28 (s, 6H, ArCH₃), 2.12-1.97 (t, $J = 6.1$ Hz, 4H, OCH₂CH₂), 1.62-1.48 (m, 4H, ArCH₂CH₂), 1.29-1.12 (m, 4H, ArCH₂CH₂CH₂CH₂CH₂), 0.83 (t, $J = 6.9$ Hz, 6H, CH₂CH₃). ¹³C NMR (75 MHz, CD₃OD) δ 159.0, 154.8, 139.9, 134.9, 132.0, 130.7, 129.9, 71.0, 40.4, 36.5, 33.2, 33.0, 31.0, 30.8, 30.1, 24.0, 16.9, 14.8. MS (ESI): calculated for [M + H - 2HCl]⁺ $m/z = 594.9$, found $m/z = 595.6$.

Bis(5-guanidine-2-hexyloxy-3-methylphenyl)methane, dichloride (25).

The pure compound was obtained as a white powder in quantitative yield.

Mp: > 250 °C dec. ¹H NMR (300 MHz, CD₃OD) δ 7.01 (d, $J = 2.6$ Hz, 2H, ArH), 6.81 (d, $J = 2.6$ Hz, 2H, ArH), 4.07 (s, 2H, ArCH₂Ar), 3.79 (t, $J = 6.4$ Hz, 4H, OCH₂), 2.31 (s, 6H, ArCH₃), 1.78 (quint, $J = 6.8$ Hz, 4H, OCH₂CH₂), 1.49 (bquint, 4H, OCH₂CH₂CH₂), 1.42-1.25 (m, 8H, OCH₂CH₂CH₂CH₂CH₂), 0.92 (t, $J = 6.9$ Hz, 6H, CH₂CH₃). ¹H NMR (300 MHz, D₂O) δ 7.13 (s, 2H, ArH), 6.90 (s, 2H, ArH), 4.06 (s, 2H, ArCH₂Ar), 3.85 (t, $J = 6.0$ Hz, 4H, OCH₂), 2.29 (s, 6H, ArCH₃), 1.76 (quint, $J = 6.6$ Hz, 4H, OCH₂CH₂), 1.50-1.23 (bs, 12H, OCH₂CH₂CH₂CH₂CH₂), 0.87 (t, $J = 6.6$ Hz, 6H, CH₂CH₃). ¹³C NMR (75 MHz, CD₃OD) δ 158.4, 156.8, 136.8, 134.9, 131.6, 128.2, 127.0, 74.4, 36.6, 33.2, 31.7, 31.3, 27.3, 24.0, 16.9, 14.7. MS (ESI): calculated for [M + H - 2HCl]⁺ $m/z = 511.4$, found $m/z = 511.7$.

X-ray Crystallographic Studies.

Crystal data, experimental details for data collection and structure refinement are reported in Table X. Intensity data and cell parameters were recorded at room temperature (293 K) on a Enraf-Nonius CAD4 diffractometer using graphite monochromated Cu-K α radiation. The intensities were corrected for Lorentz, polarization and absorption effects.

The structure was solved by Direct methods using SIR2004²⁰ and refined on F_o² by full-matrix least-squares procedures, using SHELXL-97.²¹ The structure shows a pseudo C₂ symmetry. All the non-hydrogen atoms were refined with anisotropic atomic displacements. The hydrogen atoms were included in the last cycles of the refinement at idealized geometry (C-H and N-H 0.96 Å) and refined in the “riding” model with isotropic atomic displacements 1.2 times their U_{eq} their parent atoms.

Crystal data

| | |
|---------------------------------|---|
| Empirical formula | C ₃₇ H ₃₄ N ₂ O ₆ |
| Formula weight | 602.685 |
| Crystal system | Monoclinic |
| Space group | <i>P c</i> |
| <i>a</i> (Å) | 10.389(1) |
| <i>b</i> (Å) | 12.373(1) |
| <i>c</i> (Å) | 13.047(1) |
| α (°) | 90 |
| β (°) | 108.33(1) |
| γ (°) | 90 |
| <i>V</i> (Å ³) | 1592.0(2) |
| <i>Z</i> | 2 |
| D_{calc} (g/cm ³) | 1.257 |
| <i>F</i> (000) | 636.0 |

Data collection

| | |
|-------------------------------------|---|
| Temperature (K) | 293 |
| θ Range (°) | 3.0, 70.0 (Cu-K α) |
| Index ranges | -12 $\leq h \leq$ 12 -15 $\leq k \leq$ 14 -15 $\leq l \leq$ 8 |
| Refl. measured | 3351 |
| Indep. Refl. | 3015 ($R_{int.} = 0.022$) |
| Obs. Refl. [$F_o > 4\sigma(F_o)$] | 2200 [$F_{0\geq 4\sigma(F_0)}$] |
| Data / Param. | 3015 / 408 |

Structure refinement

| | |
|---|---------------|
| Final R indices ^a | $RI = 0.144$ |
| (RI obs. Data, $wR2$ all) | $wR2 = 0.374$ |
| Goodness of Fit S^b | 1.504 |
| Min. and max. residual ρ (e/Å ³) | 1.03, -0.37 |

Table 2.1. Crystal Data and Structure Refinement for **17b**. $^aRI = \Sigma || Fo| - | Fc|| / \Sigma | Fo|$, $^bR2 = [\Sigma w(Fo^2 - Fc^2)^2 / \Sigma wFo^4]^{1/2}$. c Goodness-of-fit $S = [\Sigma w(Fo^2 - Fc^2)^2 / (n - p)]^{1/2}$, where n is the number of reflections and p the number of parameters.

DNA preparation and storage. Plasmid DNA was purified through cesium chloride gradient centrifugation.²² A stock solution of the plasmid 0.35 μ M in milliQ water (Millipore Corp., Burlington, MA) was stored at -20 °C.

Electrophoresis mobility shift assay (EMSA)

Binding reactions were performed in a final volume of 14 μ L with 10 μ L of 20 mM Tris/HCl pH 8, 1 μ L of plasmid (1 μ g of pEGFP-C1) and 3 μ L of compound at different final concentrations, ranging from 25 to 200 μ M. Binding reaction was left to take place at room temperature for 1 h; 5 μ L of 1 g/mL in H₂O of glycerol was added to each reaction mixture and loaded on a TA (40 mM Tris-Acetate) 1% agarose gel. At the end of the binding reaction 1 μ L (0.01 mg) of ethidium bromide solution is added. The gel was run for 2.5 h in TA buffer at 10 V/cm. EDTA was omitted from the buffers because it competes with DNA in the reaction.

Ethidium Bromide Displacement Assays. Fluorescence studies (excitation at 530 nm, emission at 600 nm) were performed collecting the emission spectra of buffer solutions (4 mM Hepes, 10 mM NaCl) of 50 mM ethidium bromide (relative fluorescence = 0), mixture of 0.5 nM plasmid DNA (pEGFP-C1) and 50 mM ethidium bromide (relative fluorescence = 1) and after addition of increasing amounts of guanidinium ligand.

Sample preparation and AFM imaging. DNA samples were prepared by diluting the plasmid DNA to a final concentration of 0.5 nM in deposition buffer (4 mM Hepes, 10 mM NaCl, 2 mM MgCl₂, pH = 7.4) either in the presence or absence of ligands. When needed, ethanol at a defined concentration was added to the deposition buffer prior to addition of DNA and calixarenes. The mixture was incubated for 5 min at room temperature, then a 20 μ L droplet was deposited onto freshly-cleaved ruby mica (Ted Pella, Redding, CA) for 1.5 min. The mica disk was rinsed with milliQ water and dried with a weak nitrogen stream. AFM imaging was performed on the dried sample with a Nanoscope IIIA Microscope (Digital Instruments Inc. Santa Barbara, CA) operating in tapping mode. Commercial diving board silicon cantilevers (NSC-15 Micromash Corp., Estonia) were used. Images of 512×512 pixels

were collected with a scan size of 2 μm at a scan rate of 3-4 lines per second and were flattened after recording using Nanoscope software.

Cell culture and transient transfection assay. The human rhabdomyosarcoma cell line RD-4, obtained from David Derse, National Cancer Institute, Frederick, Maryland, was maintained as a monolayer using growth medium containing 90% DMEM, 10% FBS, 2 mM l-glutamine, and 100 IU/mL penicillin, 10 $\mu\text{g}/\text{mL}$ streptomycin. Cells were subcultured to a fresh culture vessel when growth reached 70-90% confluence (i.e. every 3-5 days) and incubated at 37 $^{\circ}\text{C}$ in a humidified atmosphere of 95% air-5% CO_2 . Transfections were performed in 6 well plates, when cells were 80% confluent (approximately 3×10^5 cells) on the day of transfection. 3 μg of plasmid, and different concentration of ligands were added to 1 mL of serum-free medium, mixed rapidly and incubated at room temperature for 20 min. Each mixture was carefully added to the cells following the removal of the culture medium from the cells. Lipoplex formulations were performed adding DOPE to plasmid-ligand mixture at 1: 2 ligand: DOPE molar ratio, where ligand concentration was kept to 10 μM . LTXTM transfection reagent was used according to manufacturer's protocol as positive transfection control. The mixture and cells were incubated at 37 $^{\circ}\text{C}$ in a humidified atmosphere of 95% air-5% CO_2 for 5 h. Finally, transfection mixture was removed and 3 mL of growth medium added to each transfected well and left to incubate for 72 h. Five fields were randomly selected from each well without viewing the cells (one in the centre and one for each quadrant of the well) and examined. The transfected cells were observed under fluorescence microscope for EGFP expression. Each experiment was done three times. Statistical differences between treatments were calculated with Student's test and multifactorial ANOVA. Vero (African green monkey, ATCC CRL-1586), BoMac (bovine macrophage, obtained from J. Stabel, National Animal Disease Center, Ames, IA, USA), N2a (Mouse neuroblastoma, ATCC CCL-131), AUBEK (bovine foetal kidney cell line, ATCC CCL 163) and hMSC (human mesenchymal stem cells, obtained from R. Sala, University of Parma, Italy) were grown in EMEM medium containing NEAA, 10% FBS, 2 mM l-glutamine, 100 IU/mL penicillin and 100 $\mu\text{g}/\text{mL}$ streptomycin. All cultures were incubated at 37 $^{\circ}\text{C}$ in a humidified atmosphere containing 5% CO_2 . Transfection were performed as described for RD-4 cells.

MTT survival assay for cell viability determination. Following transfection, complete medium (90% DMEM, 10% FBS, 2 mM l-glutamine, and 100 IU/mL penicillin, 10 µg/mL streptomycin) containing MTT (5 mg/mL) was added to the culture for 4 h. Then, after the addition of an equal volume of solubilisation solution (10% SDS in HCl 0.01 M) cells were incubated at 37 °C overnight. Specific optical density was measured at 540 nm, using 690 nm as reference wavelength in an SLT-Lab microreader (Salzburg, Austria). Each experiment was done three times and each treatment was performed with eight replicates. Statistical differences among treatments were calculated with Student's test and multifactorial ANOVA.

Synthesis of 5,11,17,23-Tetra-*n*-hexyl-25,26,27,28-tetrakis(3-phthalimidopropoxy)calix[4]arene (1,3 alternate) (29).

The product was obtained according to the general procedure for the synthesis of calixarenes in 1,3-alternate conformation.²³

The crude was purified by flash column chromatography (eluent: ethyl acetate/hexane= 2.2 : 7.8 and then in CH₂Cl₂) to obtain the pure product as a colourless oil in 10% yield.

¹H NMR (300 MHz, CDCl₃) δ 7.87-7.75 (m, 8H, Pht), 7.72-7.65 (m, 8H, Pht), 6.79 (s, 8H, ArH), 4.37 (s, 8H, ArCH₂Ar), 3.62 (t, *J* = 6.9 Hz, 8H, OCH₂), 3.39 (t, *J* = 7.4 Hz, 8H, OCH₂CH₂CH₂), 2.40 (t, *J* = 7.8 Hz, 8H, ArCH₂), 1.70-1.40 (m, 16H, OCH₂CH₂ and ArCH₂CH₂), 1.35-1.12 (m, 24H, ArCH₂CH₂CH₂CH₂CH₂), 0.87 (t, *J* = 6.5 Hz, 12H, CH₃). ¹³C NMR (75 MHz, CDCl₃) δ 168.0, 154.2, 136.3, 133.7, 133.5, 132.1, 129.3, 123.1, 68.4, 37.8, 35.4, 35.1, 31.7, 31.6, 29.4, 28.8, 22.7, 14.1. MS (ESI): calculated for [M + Na]⁺ *m/z* = 1531.8, found *m/z* = 1532.4.

Synthesis of 5,11,17,23-Tetra-*n*-hexyl-25,26,27,28-tetrakis(3-aminopropoxy)calix[4]arene (1,3-alternate) (29). The product was obtained according to a general procedure for the removal of the phthaloyl protecting groups, mentioned above for **2c**.

The pure compound was obtained as a colourless oil in quantitative yield.

¹H NMR (300 MHz, CDCl₃) δ 6.89 (s, 8H, ArH), 3.77 (bs, 8H, ArCH₂Ar), 3.60 (bs, 8H, OCH₂), 2.62 (bs, 8H, OCH₂CH₂CH₂), 2.56 (bs, 8H, ArCH₂), 1.57 (bs, 16H, OCH₂CH₂ and ArCH₂CH₂), 1.25 (bs, 24H, ArCH₂CH₂CH₂CH₂CH₂), 0.83 (bs, 12H, CH₃). ¹³C NMR (75 MHz, CDCl₃) δ 154.7, 136.3, 133.7, 131.1, 129.5, 125.5, 68.9, 39.2, 38.3, 35.3, 31.7, 31.6, 29.6, 29.3, 22.5, 14.0. MS (ESI): calculated for [M + H]⁺ *m/z* = 989.9, found *m/z* = 989.8, calculated for [M + Na]⁺ *m/z* = 1011.8, found *m/z* = 1011.5.

General procedure for the reaction of amines with CO₂

CO₂(g) was bubbled with a needle through a solution of the amine (~ 1-10 mM) in the deuterated solvent in the NMR tube for 7-10 min. NMR spectra were recorded immediately after the bubbling.

Adduct 28.

The compound was obtained as a white solid in quantitative yield.

¹H NMR (300 MHz, CDCl₃): δ 9.35 (bs, 6H, NH₃⁺), 7.17 (d, *J* = 7.4 Hz, 4H, Ar*H*), 7.00 (t, *J* = 7.4 Hz, 2H, Ar*H*), 6.20 (t, *J* = 7.5 Hz, 2H, Ar*H*), 6.06 (d, *J* = 7.5 Hz, 4H, Ar*H*), 4.74 (bt, 2H, NHCOO⁻), 4.33 (d, *J* = 13.2 Hz, 4H, ArCH₂Ar), 4.08 (t, *J* = 7.5 Hz, 4H, OCH₂CH₂CH₂NH₃⁺), 3.66 (bs, 8H, OCH₂CH₂CH₂NHCOO⁻ and OCH₂CH₂CH₂NHCOO⁻), 3.17 (d, *J* = 13.2 Hz, 4H, ArCH₂Ar), 2.85 (bs, 4H, OCH₂CH₂CH₂NH₃⁺), 2.41 (bs, 4H, OCH₂CH₂CH₂NH₃⁺), 1.95 (bs, 4H, OCH₂CH₂CH₂NHCOO⁻). ¹H NMR (300 MHz, DMSO-*d*₆): δ 6.76 (bs, 4H, NH), 6.63-6.50 (m, 12H, Ar*H*), 4.30 (d, *J* = 13.0 Hz, 4H, ArCH₂Ar), 3.85 (bs, 8H, OCH₂), 3.14 (d, *J* = 13.0 Hz, 4H, ArCH₂Ar), 3.12 (bs, CH₂NHCOOH), 2.02 (bs, 8H, OCH₂CH₂). ¹³C NMR (75 MHz, CDCl₃): δ 163.6, 156.3, 154.2, 137.2, 132.6, 129.2, 127.6, 122.8, 122.3, 74.3, 72.5, 41.1, 36.4, 32.3, 30.2, 27.3. ¹³C NMR (75 MHz, DMSO-*d*₆): δ 157.5, 155.7, 134.4, 127.8, 121.7, 72.5, 37.2, 30.3, 30.1.

Adduct 31.

The compound was obtained as a white solid in quantitative yield.

¹H NMR (300 MHz, CDCl₃): δ 7.93 (bs, 3H, NH₃⁺), 6.98 (s, 2H, Ar*H*), 6.94 (s, 1H, Ar*H*), 6.83 (s, 1H, Ar*H*), 4.88 (bs, 1H, NHCOO⁻), 3.98 (s, 2H, ArCH₂Ar), 3.78 (bs, 2H, OCH₂CH₂CH₂NHCOO⁻), 3.56 (bs, 2H, OCH₂CH₂CH₂NH₃⁺), 3.31 (bs, 2H, OCH₂CH₂CH₂NHCOO⁻), 3.11 (bs, 2H, OCH₂CH₂CH₂NH₃⁺), 2.23 (s, 3H, ArCH₃), 2.20 (s, 3H, ArCH₃), 2.12 (bs, 2H, OCH₂CH₂CH₂NH₃⁺), 1.90 (bs, 2H, OCH₂CH₂CH₂NHCOO⁻), 1.22 (s, 9H, *t*Bu), 1.17 (s, 9H, *t*Bu). ¹³C NMR (75 MHz, CDCl₃): δ 163.6, 152.9, 152.7, 146.1, 146.0, 132.7, 132.3, 129.8, 126.0, 125.9, 124.9, 71.4, 69.4, 39.7, 37.1, 34.1, 31.3, 31.1, 29.6, 29.1, 28.9, 16.5.

2.6 References

[§]Part of the results reported in this chapter have been already published: see ref. 6a.

1. a) Fernandez-Carneado, J.; Van Gool, M.; Martos, V.; Castel, S.; Prados, P.; de Mendoza, J.; Giralt, E. *J. Am. Chem. Soc.* **2005**, *127*, 869-874; b) Takeuchi, T.; Kosuge, M.; Tadokoro, A.; Sugiura, Y.; Nishi, M.; Kawata, M.; Sakai, N.; Matile, S.; Futaki, S. *ACS Chemical Biology* **2006**, *1*, 299-303; c) Wender, P. A.; Wesley C. G.; Goun, E. A.; Jones, L. R.; Pillow, T. H. *Advanced Drug Delivery Reviews* **2008**, *60*, 452-472.
2. Sansone, F.; Dudic, M.; Donofrio, G.; Rivetti, C.; Baldini, L.; Casnati, A.; Cellai, S.; Ungaro, R. *J. Am. Chem. Soc.* **2006**, *128*, 14528-14536.
3. a) Wasungu, L.; Hoekstra, D. *J. Controlled Release* **2006**, *116*, 255-264; b) Farhood, H.; Serbina, N.; Huang, L. *Biochim. Biophys. Acta* **1995**, *1235*, 289-295.
4. Marron, B. E.; Spanevello, R. A.; Elisseou, M. E.; Serhan, C. N.; Nicolaou, K. C. *J. Org. Chem.* **1989**, *54*, 5522-5527.
5. Shinkai, S.; Nagasaki, T.; Iwamoto, K.; Ikeda, A.; He, G.-X.; Matsuda, T.; Iwamoto, M. *Bull. Chem. Jpn.* **1991**, *64*, 381-386.
6. a) Bagnacani, V.; Sansone, F.; Donofrio, G.; Baldini, L.; Casnati, A.; Ungaro, R. *Org. Lett.* **2008**, *10*, 3953-3956; b) Barbosa, S.; Garcia Carrera, A.; Matthews, S. E.; Arnaud-Neu, F.; Böhmer, V.; Dozol, J.-F.; Rouquette, H.; Schwing-Weill, M.-J. *J. Chem. Soc., Perkin Trans. 2* **1999**, *4*, 719-723; c) Casnati, A.; Della Ca', N.; Fontanella, M.; Sansone, F.; Ugozzoli, F.; Ungaro, R.; Liger, K.; Dozol, J.-F. *Eur. J. Org. Chem.* **2005**, *11*, 2338-2348.
7. Masayoshi, A.; Nakashima, K.; Kawabata, H.; Tsutsui, S.; Shinkai, S. *J. Chem. Soc. Perkin. Trans. 2* **1993**, 347-354.
8. Casiraghi, G.; Casnati, G.; Cornia, M.; Pochini, A.; Sartori, G.; Ungaro, R. *J. Chem. Soc. Perkin Trans. 1* **1978**, *4*, 322-325.
9. Dudic, M.; Colombo, A.; Sansone, F.; Casnati, A.; Donofrio, G.; Ungaro, R. *Tetrahedron* **2004**, *60*, 11613-11618.
10. Borovik, A. S.; Kalambet, Y. A.; Lyubchenko, Y. L.; Shitov, V. T.; Golovanov, E. I. *Nucleic Acid Res.* **1980**, *8*, 4165-4184.
11. Bustamante, C.; Rivetti, C. *Annu. Rev. Biophys. Biomol. Struct.* **1996**, *25*, 395-429; b) Hansma, H. G. *Annu. Rev. Phys. Chem.* **2000**, *52*, 71-92.
12. Martin, A. L.; Davies M. C.; Rackstraw, B. J.; Roberts, C. J.; Stolnik, S.; Tendler, S. J. B.; Williams, P. M. *FEBS Letters* **2000**, *480*, 106-112.
13. Lipofectamine LTX Reagent is a cationic lipid-based, animal-origin free formulation for the transfection of DNA into eukaryotic cells with low cytotoxicity. See: http://www.invitrogen.com/downloads/F-069843-LpofctLTX_FHR.pdf.

14. a) Kostarelos, K.; Miller, A. D. *Chem. Soc. Rev.* **2005**, *34*, 970-994; (b) Boeckle, S.; Wagner, E. *AAPS J.* **2006**, *8*, 731-742; (c) Zuhorn, I. S.; Engberts, J. B. F. N.; Hoekstra, D. *Eur. Biophys. J.* **2007**, *36*, 349-362.
15. Goun, E. A.; Pillow, T. H.; Jones, L. R.; Rothbard, J. B.; Wender, P. A. *Chembiochem* **2006**, *7*, 1497-1515.
16. *Nature* **2008**, *455*, 581.
17. a) Xu, H.; Rudkevich, D. M. *J. Org. Chem.* **2004**, *69*, 8609-8617; b) Xu, H.; Rudkevich, D. M. *Chem. Eur. J.* **2004**, *10*, 5432-5442.
18. C. Gutsche, D.; Bauer, L. J. *J. Am. Chem. Soc.*, **1985**, *107*, 6052-6059.
19. Kenis, P. J. A.; Noordman, O. F. J.; Schönherr, H.; Kerver, E. G.; Snellink-Ruël, B. H. M.; van Hummel, G. J.; Harkema, S.; van der Vorst, C. P. J. M.; Hare, J.; Picken, S. J.; Engbersen, J. F. J.; Vancso, G. J. *Chemistry, a European Journal* **1998**, *4*, 1225-1234.
20. Mislin, G.; Graf, E.; Hosseini, M. W. *Tetrahedron Lett.* **1996**, *37*, 4503-4506.
20. Burla, M. C.; Caliandro, R.; Camalli, M.; Carrozzini, B.; Cascarano, G. L.; De Caro, L.; Giacovazzo, C.; Polidori, G.; Spagna, R. *J. Appl. Cryst.* **2005**, *38*, 1381-1388.
21. Sheldrick, G. M. **SHELX-97**, *Program for Crystal Structure Refinement*, University of Göttingen, 1997; <http://shelx.uni-ac.gwdg.de/shelx/index.html>.
22. Maniatis, T.; Fritsch, E. F.; Sambrook, J. in *Molecular Cloning: A Laboratory Manual*, 2nd edition, **1989**, Cold Spring Harbor Laboratory: New York.
23. Crenguta, D.; Bolte, M.; Böhmer, V. *Org. Biomol. Chem.* **2005**, *3*, 172-184.